Original Article

POTENTIAL OF NOTOCHORDAL CELLS WITHIN INJECTABLE BIOMATERIALS TO PROMOTE INTERVERTEBRAL DISC REGENERATION

R.J. Williams[1,2], S. Basatvat[1,2], T.C. Schmitz[3], R. Janani[4], C. Sammon[4], K. Benz[5], K. Ito[3], M.A. Tryfonidou[6], J.W. Snuggs[1,2] and C.L. Le Maitre[1,2,*]

[1]Division of Clinical Medicine, School of Medicine and Population Health, University of Sheffield, S10 2RX Sheffield, UK
[2]Biomolecular Sciences Research Centre, Sheffield Hallam University, S1 1WB Sheffield, UK
[3]Orthopaedic Biomechanics, Department of Biomedical Engineering, Eindhoven University of Technology, 5612 AZ Eindhoven, The Netherlands
[4]Materials Engineering Research Institute, Sheffield Hallam University, S1 1WB Sheffield, UK
[5]TETEC Tissue Engineering Technologies AG, 72770 Reutlingen, Germany
[6]Department of Clinical Sciences, Faculty of Veterinary Medicine, Utrecht University, 3584 CS Utrecht, The Netherlands

Abstract

Low back pain is the leading cause of disability worldwide and is strongly associated with degeneration of the intervertebral disc (IVD). During degeneration the nucleus pulposus (NP) in the core of the IVD, is affected by altered matrix synthesis, increased degradation, and cell loss. Strategies combining regenerative cell sources with injectable biomaterials could provide a therapeutic approach to treating IVD-degeneration related back pain. The juvenile cells of the NP, known as notochordal cells (NC), could provide both anabolic and anti-catabolic responses for disc regeneration. However, their behaviour within biomaterial delivery systems has not been investigated. Here, porcine NCs were incorporated into three injectable hydrogels: Albugel (an albumin/hyaluronan hydrogel), NPgel (a L-pNIPAM-co-DMAc hydrogel) and NPgel with decellularized NC-matrix powder (dNCM). The NCs and biomaterial constructs were cultured for up to 4 weeks under 5 % oxygen (n = 3 biological repeats). The ability of biomaterials to maintain NC viability, phenotype and extracellular matrix synthesis and deposition was investigated through histological, immunohistochemical and glycosaminoglycans analysis. NCs survived in all three biomaterials after 4 weeks, whilst phenotype and cell clustering were maintained to a greater extent in NPgel and Albugel. Thus, these biomaterials could facilitate maintenance of the NC phenotype, support matrix deposition and be a basis for future IVD regeneration strategies.

Keywords: IVD degeneration, disc degeneration, biomaterial, notochordal cells, hydrogels, hyaluronic acid.

***Address for correspondence**: C.L. Le Maitre, Division of Clinical Medicine, School of Medicine and Population Health, The University of Sheffield, S10 2RX Sheffield, UK. Email: c.lemaitre@sheffield.ac.uk

Copyright policy: © 2024 The Author(s). Published by Forum Multimedia Publishing, LLC. This article is distributed in accordance with Creative Commons Attribution Licence (http://creativecommons.org/licenses/by/4.0/).

Introduction

Lower Back Pain and Intervertebral Disc Degeneration

Low back pain (LBP) is the biggest cause of disability worldwide; around 80 % of adults will suffer from LBP in their lifetime (Hartvigsen *et al.*, 2018; Traeger *et al.*, 2019). Most people experience mild pain and recover quickly, however, in some cases LBP lasting longer than 6 weeks progresses to chronic LBP (CLBP) which can contribute to lifelong disability and societal burden (Hartvigsen *et al.*, 2018; Maetzel & Li, 2002). Current treatments to combat LBP may be pharmacological or non-pharmacological, such as: non-steroidal anti-inflammatory drugs, opioids, anti-depressants, exercise, massage, and manipulation (NICE, 2020; Qaseem *et al.*, 2017). Whilst CLBP can be tackled with surgery in some situations, but this is invasive, expensive, and only targets the end-stage of disease in the spine having limited effectivity to manage CLBP in many patients (Bogduk, 2004; Foster *et al.*, 2018; Phillips *et al.*, 2003; Steffens *et al.*, 2016). In around 40 % of cases, the underlying cause of CLBP is associated with degeneration of the intervertebral disc (IVD) (Luoma *et al.*, 2000; Sakai & Andersson, 2015). Importantly, none of the current treatments target the regeneration of the IVD.

Intervertebral Disc and Notochordal Cells

The IVD permits range of motion and supports biomechanical forces applied to the spine (Risbud & Shapiro,

2011). The core of the disc contains an aggrecan-rich gel-like tissue called the nucleus pulposus (NP), which is enclosed circumferentially by the ligamentous annulus fibrosus (AF). The composition of the NP changes as a human IVD matures. The NP of a neonate is populated by notochordal (NC) cells, which are large, vacuolated, and morphologically distinct cells. In humans, some canine breeds, and other species, such as ovine and caprine, large vacuolated NCs (morphotypic NCs) gradually disappear during disc maturation, substituted by more smaller NP cells as the primary cell type (Bach *et al.*, 2022; Sheyn *et al.*, 2019). However, certain species retain morphotypic NCs within the NP region throughout most of their lifespan, including porcine, leporine, and murine species (Alini *et al.*, 2008; Sheyn *et al.*, 2019). Interestingly, an association between morphotypic NC loss and the onset of disc degeneration has been highlighted, where natural degeneration is only seen in species which lose their morphotypic NCs prior to adulthood (Bergknut *et al.*, 2012; McCann & Séguin, 2016; Jill P.G. Urban & Roberts, 2003). As a result, NCs have become a trending research topic regarding their promise for therapeutic application to mediate disc regeneration (Bach *et al.*, 2022; Humphreys *et al.*, 2018).

Regenerating the Intervertebral Disc with Cell-biomaterial Treatments

Of the cell types which have been considered for the purposes of regenerating a degenerative IVD, less than 3 % of the papers utilised NCs as the choice of regenerative cell source in a recent review (Williams *et al.*, 2021). The review highlights that NCs have been successfully extracted from several species, however, these studies have mainly focused on 3D *in vitro* culture, with a distinct lack of progression into *in vivo* studies (Williams *et al.*, 2021). The limited use in studies so far may have been due to the difficulties in NC handling, such as: the inability to maintain their phenotype in monolayer culture (Gantenbein *et al.*, 2014; Potier & Ito, 2014; Spillekom *et al.*, 2014), harvesting insufficient numbers due to limited amplification and inability to passage whilst maintaining phenotype (Kim *et al.*, 2009; Potier *et al.*, 2014; Spillekom *et al.*, 2014; Williams *et al.,* 2023). Nonetheless, NCs could provide an excellent cell source for regenerating the degenerate IVD, due to their capabilities of synthesising extracellular matrix, being highly viable in the conditions within the IVD and producing anti-angiogenic, and anti-catabolic effects (Gantenbein *et al.*, 2014; Potier *et al.*, 2014; Purmessur *et al.*, 2013; Spillekom *et al.*, 2014), for a recent review on the potential of NCs please see Bach *et al.* (2022).

The limitation of NCs being maintained only in 3D culture models can be addressed by the seeding of cells directly into a biomaterial scaffold, facilitating cell growth and/or favourable differentiation, to provide mechanical support and aid the delivery of the cells into the disc (Peroglio *et al.*, 2012; Thorpe *et al.*, 2016). A proposed biomaterial that enables liquid injection followed by *in situ* gelation, with additional attributes of biocompatibility, mechanical stability, compliance with regulatory pathway approvals and facile translation from research to future medical application, would be an ideal candidate for a therapeutic treatment.

Hydrogel-based biomaterial carriers that have previously been developed for NP regeneration, were investigated in this study to support NCs. The first biomaterial selected was a polyethylene glycol-crosslinked serum albumin/hyaluronan hydrogel, referred to as Albugel, which has been previously shown to support the survival of disc cells and disc healing and has been shown safe to use in human clinical trials regarding cartilage therapy in knee joints (Benz *et al.*, 2010, 2012; Niemeyer *et al.*, 2022). The second selected biomaterial was a synthetic Laponite® crosslinked poly N-isopropylacrylamide-co-N, N-dimethylacrylamide (NPgel) biomaterial (Boyes *et al.*, 2021) which has been previously reported to induce human bone marrow progenitor cell differentiation into an NP-like phenotype with matrix deposition that mimics the native NP tissue (Thorpe *et al.*, 2016; Thorpe *et al.*, 2017; Vickers *et al.*, 2019), and can restore degenerate discs in a goat organ culture model (Snuggs *et al.*, 2023). The importance of cells to retain their NP phenotype will facilitate the regenerative potential of the cells, such as NP cell production of extracellular matrix. This hydrogel system has also undergone *in vivo* safety studies in rats, where it was demonstrated to not show any adverse events within a subcutaneous implantation model (Thorpe *et al.*, 2018). The third and final biomaterial was selected to investigate whether the inclusion of the native extracellular matrix from the NC-rich NP tissue improved phenotypic maintenance. Notochordal cell matrix (NCM)-based materials have been previously shown to promote anabolism within NP cells and degenerated IVD tissue (De Vries *et al.*, 2019; Schmitz *et al.*, 2022). Thus, here the hypothesis that the supplementation of the synthetic NPgel with the NCM would provide additional cues to the NCs supporting their phenotype (Bach *et al.*, 2018; Bai *et al.*, 2017; Cornejo *et al.*, 2015; Vickers *et al.*, 2019), specifically a decellularised NCM (dNCM) was utilised creating a bioactive functional biomaterial (NPgel/dNCM).

Altogether, this study investigated the use of porcine NCs (pNCs) in combination with three potential injectable biomaterials: Albugel, NPgel and NPgel/dNCM that were intentionally representative of either synthetic (NPgel), semi-synthetic (NPgel/dNCM) or primarily based on natural components (Albugel), as a first translation step of NC-based therapeutic strategies.

Materials and Methods

Experimental Design

To ensure biomaterials to be tested further with cell studies could withstand the shear stresses within the native

disc, initial preliminary rheological characterisation was performed, biomaterials which failed to withstand these forces would be excluded from further study. Optimisation experiments were then performed by seeding pNCs into a readily available biomaterial, which has been extensively characterised (NPgel) (Boyes *et al.*, 2021; Thorpe *et al.*, 2016; Thorpe *et al.*, 2017; Vickers *et al.*, 2019). These initial optimisation studies were used to determine optimal seeding density, and viability. Thereafter, pNCs were harvested from three independent biological porcine donors, the discs from each donor were pooled together prior to seeding into three different injectable biomaterials in at least duplicate per donor, total replicates: Albugel (n = 8), NPgel (n = 8) and NPgel/dNCM (n = 6), with all output measures performed on every sample. Cell-biomaterial constructs were cultured for 4 weeks in IVD conditions in relation to physioxia and low glucose conditions. Following culture viability was assessed using Calcein/Hoechst staining. Morphology and porous structure of the gel networks were investigated using scanning electron microscopy (SEM) and histology. Finally, phenotype and matrix production was assessed using immunohistochemistry and histological staining.

NPgel Preparation

Laponite® crosslinked pNIPAM-co-DMAc (NPgel) biomaterial was prepared as previously described (Thorpe *et al.,* 2016). In short, a 10 mL exfoliated suspension of 0.11 g Laponite® clay nanoparticles (25-30 nm diameter, $<$ 1 nm thickness) (BYK Additives Ltd, Widnes, UK) in 18 mΩ deionized H_2O was prepared. To the 10 mL exfoliated Laponite® clay suspension, 0.87 g N-isopropylacrylamide 99 % (NIPAM) (KJ Chemicals, Tokyo, Japan), 0.13 g N-dimethylacrylamide (DMAc) (274135; Sigma, Dorset, UK), and 0.01 g 2-20-azobisisobutyronitrile (AIBN) (441090; Sigma, Dorset, UK) were added, mixed well, and filtered through a 5 to 8 µm pore filter paper. Polymerization was performed at 80 °C overnight. NPgel suspension was cooled to ~38-39 °C prior to cell incorporation.

NPgel with dNCM Preparation

Decellularized NCM powder (dNCM) was prepared as previously described (Schmitz *et al.,* 2022). Briefly, NC-rich NP tissue was harvested from 12-week-old porcine donors and processed by firstly freeze drying in a lyophilizer (Labconco, Kansas City, MO, USA) overnight at – 80 °C, then for $>$ 7 hours at $\leq$ – 50 °C. The sample was then decellularized using a 200 U/mL benzonase (E1014; Merck KGaA, Darmstadt, Germany) in 50 mM Tris-HCl buffer (93313; Sigma, Zwijndrecht, The Netherlands), pH 7.5, 2.5 mM $MgCl_2$ (M8266; Sigma, Zwijndrecht, The Netherlands) at 0.01 mL buffer/mg dry weight tissue for 48 hours at 37 °C on a roller at 2 rpm; followed by pulverization to obtain a powder that can be kept a – 80 °C. The dNCM was then sterilized using UV light and 0.5 % w/v was stirred to be dispersed within NPgel just prior to cell seeding, a single batch of dNCM was utilised for these studies.

Albugel Preparation

Albugel (an albumin/hyaluronan hydrogel) was prepared by firstly creating hyaluronic acid (HA) solution; HA solution was constructed with 35 % v/v Ostenil Plus® (TRB Chemedica, Newcastle-under-Lyme, UK) and alpha Minimum Essential Medium (α-MEM, 12571063; Gibco™ Life Technologies, Paisley, UK) base media. This was then combined with 11 % v/v chemically modified human serum albumin (maleimido-human serum albumin; MA-HSA; TETEC, Germany), 18 % v/v cell suspension. Using a dual syringe with a mixing head, the HA, MA-HSA and cell mixture was combined with the crosslinker α,ω-bisthio-polyethylene glycol (BT-PEG; Laysan Bio Inc. Arab, AL, USA) at 1:5 ratio.

Rheological Characterisation

The rheological behaviour of the biomaterials at different degrees of deformation was characterised using an Anton Paar 301 rheometer (Anton Paar, Graz, Austria) in parallel plates configuration. Circular samples were prepared using bespoke Polytetrafluoroethylene (PTFE) moulds (20 mm in diameter, 2 mm in height) and immersed in low glucose Dulbecco's modified eagles media (DMEM, 10567014; Gibco™ Life Technologies, Paisley, UK), with pyruvate pH adjusted to 6.8 to mimic the degenerate disc environment for up to 24 hours at 37 °C. To prevent sample slippage during measurement, sandpaper was attached to the measuring plates. A constant load of 1 N was applied on the sample throughout the measurement to maintain good contact between the sample and the top plate. Amplitude sweep measurements were conducted on the hydrogel samples between 0.1-50 % strain at 1 Hz frequency after 2 and 24 hours of immersion in media. A minimum of three replicates were conducted for each sample and the average moduli values are reported here. For samples that suffered from shrinkage, the resultant moduli values were corrected by the factor $(\frac{d}{d_{sample}})^4$ where d is the diameter of the upper plate and d_{sample} is the diameter of the measuring sample (Bron *et al.,* 2009).

Notochordal Cell Extraction

pNC were obtained from lumbar IVDs harvested from young pigs ($<$ 15 weeks old) (Medical Meat supplier, Rochdale, UK and Marr Grange Butchers, Doncaster, UK). Following the protocol from Williams *et al.* (2023), the spines were dissected, and the NP harvested under sterile conditions, the NP tissue from the same porcine donor were pooled and digested following a sequential treatment in 7 U/mL pronase (PRON-RO; Sigma, Dorset, UK) in α-MEM modified with ribonucleosides, deoxyribonucleosides, phe-

nol red, L-glutamine (12571063; Gibco™ Life Technologies, Paisley, UK) with 1 % v/v Penicillin-Streptomycin (P/S, 15140122; Gibco™ Life Technologies, Paisley, UK) for 30 minutes at 37 °C. Followed by a 16 hour digestion in 125 U/mL collagenase type II (17101015; Gibco™ Life Technologies, Paisley, UK) in α-MEM at 37 °C. The clusters of pNC were captured in a 40 µm cell strainer and further cultured as described below.

Incorporation of Notochordal Cells into Biomaterials and Culture

pNC clusters were counted post harvesting using a NucleoCounter® NC-200™ (Chemometec, Allerod, Denmark), as previously described in Williams *et al.* (2023). For seeding, harvested pNC were centrifuged at 300 g for 5 minutes, the supernatant was removed, and the NC pellet was resuspended in αMEM (12571063; Gibco™ Life Technologies, Paisley, UK) containing P/S 50 U/mL (15140122; Gibco™ Life Technologies, Paisley, UK), prior to adding the biomaterials to the Eppendorf. Cell density optimisation studies investigated 1×10^6, 4×10^6, 1×10^7 and 2×10^7 cells/mL within NPgel for 2 weeks in culture. From which a final cell density of 4×10^6 cells/mL of pNC was selected for further studies and seeding into the three injectable biomaterials: Albugel, NPgel and NPgel/dNCM. In addition, parallel acellular biomaterial controls were established. Each 300 µL pNC and biomaterial constructs were extruded through a 27 gauge needle to mimic injection into the disc into 48 well culture plate, left to gel at 37 °C for 5 minutes. Five hundred microliters of complete NC culture media was then added to the well: α-MEM (12571063; Gibco™ Life Technologies, Paisley, UK) containing P/S 50 U/mL (15140122; Gibco™ Life Technologies, Paisley, UK), amphotericin B 2.5 µg/mL (A2942; Sigma, Dorset, UK), L-ascorbic acid 25 µg/mL (A4403; Sigma, Dorset, UK), 1 % Insulin-transferrin-Selenium v/v (ITS-X, 51500056; Gibco™ Life Technologies, Paisley, UK), 1 % L-glutamine v/v (25030081; Gibco™ Life Technologies, Paisley, UK), L-proline 40 µg/mL (A10199-22; Gibco™ Life Technologies, Paisley, UK) and Albumax 1.25 mg/mL (11021037; Gibco™ Life Technologies, Paisley, UK) (Basatvat *et al.*, 2023), leaving the outer wells of the plate void of constructs, but hydrated with phosphate buffered saline (PBS, 10010023; Gibco™ Life Technologies, Paisley, UK). Triplicate biological repeats of cellular and acellular controls were cultured for up to 4 weeks in a physiological disc environment of 5 % v/v O_2, with5 % v/v CO_2 at 37 °C using a hypoxia glove box (Coy Laboratory Products, Grass Lake, MI, USA). Complete media was replaced in the hypoxia glove box three times per week during the culture period.

To assess initial cell viability, constructs were stained with 10 µM Calcein-AM (C1430; Invitrogen™, Carlsbad, CA, USA) and Hoechst 33342 (H3570; Invitrogen™, Carlsbad, CA, USA). Constructs following culture were firstly washed in PBS, next, cells were stained with 10 µM of Calcein-AM for 30 minutes at 37 °C, washed three times with PBS, followed by 5 pg/mL of Hoechst for 15 minutes at 37 °C. After staining culture media was re-added, and a small piece of the construct was taken and constrained between a microscope slide and coverslip and visualised on an Olympus BX60 microscope (Olympus Life Science, Southend-on-Sea, UK) using 494 nm filter (fluorescein isothiocyanate (FITC)) and 361 nm filter (4,6-diamidino-2-phenylindole (DAPI)) for visualising Calcein-AM and Hoechst stains, respectively. After the culturing for up to 3 weeks constructs were harvested for assessment of cell morphology, matrix deposition and analysis of cellular phenotypic markers, along with acellular controls.

Scanning Electron Microscopy

Triplicate samples were removed from culture and flash frozen with liquid $N_2$and stored at – 80 °C. The samples were freeze dried overnight using a freeze dryer (FD-1A-50; Boyikang, Beijing, China) at – 50 °C under vacuum. The samples were then fractured to expose the interior surface morphology, attached onto an aluminium stub, and then using a Quorum Technology 150 Q TES system (Quorum Technology, East Sussex, UK) (FEI NOVA, Oregon, USA). Secondary electron images were obtained using accelerating voltage 5 kV at various magnifications ranging from 600× to 6,000×.

Histological Analysis

NC phenotype and matrix deposition was investigated in acellular controls and cellular constructs following 2 and 4 weeks in culture. Triplicate samples per biomaterial were removed from culture and fixed in 10 % w/v neutral buffered formalin for 20 minutes and processed to wax using the TP1020 tissue processor (Leica Microsystems, Newcastle, UK). Following fixing and embedding, all samples were sectioned at 6 µm and mounted to X-tra® adhesive positively charged slides (Leica Microsystems, Newcastle, UK). Sections were dewaxed in Sub X (Leica Microsystems, Newcastle, UK) three times for 7 minutes and rehydrated in industrial methylated spirit (IMS; Fisher, Loughborough, UK; 10552904) for three times for 7 minutes and hydrated in running tap water for 5 minutes prior to histological staining. Sections were assessed using histological stains. Haematoxylin & Eosin (H&E): Mayer's Haematoxylin (MHS32; Sigma, Dorset, UK) for 1 minute, before being 'blued' in running water for 5 minutes and immersed in Eosin (3801601; Leica Microsystems, Newcastle, UK) for a further 1 minute; Alcian Blue (pH 2.5, 38016SS3; (Leica Microsystems, Newcastle, UK) for 30 minutes;) followed by counter stain of Nuclear fast red (38016SS3; Leica Microsystems, Newcastle, UK) for 10 minutes; Masson's Trichrome (RRSK20; Atom Scientific, Manchester UK): according to the manufacturer's instructions; Safranin O/Fast green: sections are stained with

Weigert's Haematoxylin for 5 minutes, followed by 0.4 % v/v aqueous Fast green (F7252; Sigma, Dorset, UK) for 4 minutes, rinsed with 1 % v/v acetic acid (695092; Sigma, Dorset, UK) and counter stained with 0.125 % w/v Safranin O (S2255; Sigma, Dorset, UK). After specific histological staining, sections were dehydrated three times for 10-minute washes in IMS, cleared in Sub-X (3803670E; Leica Microsystemcs, Newcastle, UK) three times for 10-minute and mounted in Pertex (3808707E; Leica Microsystems, Newcastle, UK). All slides were examined with an Olympus BX51 microscope and images captured by digital camera and Capture Pro OEM v8.0 software (Media Cybernetics, UK). Histological sections were analysed, and representative images captured to document their histological appearance and cellular staining patterns.

Immunohistochemistry and Immunofluorescence Analysis

Immunohistochemistry (IHC) and immunofluorescence were also performed on porcine disc samples and pNCs cultured in biomaterials. Specific antibodies were used to target antigens in relation to NP matrix, NC and NP phenotype (Table 1). Samples embedded in paraffin wax were dewaxed in Sub X for three times for 7 minutes and rehydrated in IMS for three times for 7 minutes. For IHC, as previously reported (Binch *et al.*, 2020), endogenous peroxidase activity was blocked for 30 minutes using IMS containing 3 % w/w H_2O_2 (8.22287; Sigma, Dorset, UK) and 5 drops of 37 % hydrochloric acid. Followed by three times for 5 minutes washes in tris-buffered saline (TBS; 20 mM tris (10528830; Fisher, Loughborough, UK), 150 mM sodium chloride (10092740; Fisher, Loughborough, UK), pH 7.5). Sections were subjected to antigen retrieval methods as detailed in Table 1. For heat antigen retrieval, sections were immersed in pre-heated (60 °C) antigen retrieval buffer (0.05 M tris, pH 9.5) and irradiated for 5 minutes at 40 % power in a microwave oven (Sanyo 800 Watt) and then again for 5 minutes at 20 % power. Sections were left to stand at room temperature for 15 minutes. For enzyme antigen retrieval, sections were placed in a pre-heated (37 °C) TBS buffer with 0.01 % w/v α-chymotrypsin (C4129; Sigma, Dorset, UK) in 0.1 % w/v $CaCl_2$ for 30 minutes at 37 °C; or no retrieval was required. Sections were washed in TBS and blocked for 2 hours with normal serum from which the animal in which the secondary antibody was raised in; 5 % v/v bovine serum albumin (BSA, A7030; Sigma, Dorset, UK) w/v in 75 % TBS and 25 % normal serum v/v (Table 1). Primary antibody was applied overnight at 4 °C according to Table 1 alongside equivalent concentration IgG controls. On the second day, the sections were washed in TBS followed by appropriate biotinylated secondary antibody for 30 minutes. Sections were subject to avidin-biotin-complex (ABC) elite reagent for 30 minutes (PK-7100; Vector Laboratories, Newark, CA, USA), 3,3-diaminobenzidine tetrahydrochloride (DAB) solution (D5637; Sigma, Dorset, UK) for 20 minutes and washed in running tap water for 5 minutes prior to counterstaining with Mayer's Haematoxylin for 1 minute and blued in running tap water for 5 minutes. Sections were dehydrated in IMS three times for 10 minutes, cleared in Sub-X three times for 10 minutes, and mounted in Pertex.

Dimethylmethylene Blue Assay

Media samples were collected during every media change during the culture of the pNC in biomaterial constructs and stored at – 80 °C. Dimethylmethylene blue (DMMB) reagent was generated with 1,9-dimethylmethylene blue (341088; Sigma, Dorset, UK), formic acid (F0507; Sigma, Dorset, UK), and sodium formate (247596; Sigma, Dorset, UK), adjusted to pH 6.8 and diluted so that the optical density (OD) measured between 0.38 and 0.41 with a blank sample. Once ready to perform a DMMB assay, media was thawed at room temperature, 50 µL of construct sample was added to 96 well plate (167425; Thermofisher, Waltham, MA, USA) followed by 20 µL of guanidinium chloride solution (2.16 M Guanidium Chloride (1.0422; Sigma, Dorset, UK) diluted in papain buffer (0.1 M sodium acetate (76728; Sigma, Dorset, UK), 0.01 M L-cysteine hydrochloride (C1276; Sigma, Dorset, UK), 0.05 M disodium EDTA (E5134; Sigma, Dorset, UK), 0.2 M NaCl (S9888; Sigma, Dorset, UK)) adjusted to pH 6.0), adjusted to pH 6.8, followed by 200 µL of DMMB reagent. The plate was set to orbital shake for 5 seconds followed by a 3 minutes rest before being read at 520 nm absorption using a CLARIOstar®Microplate Reader (BMG Labtech, Aylesbury, UK).

Statistical Analysis

Statistics were performed in GraphPad prism v8.4.1 (GraphPad Software, Inc., San Diego, CA, USA). The normality of the data was assessed using the Shapiro-Wilk test. The cell distribution when seeded within the biomaterials was not normally distributed, therefore analysed with a Kruskal-Wallis test followed by the Dunn's multiple comparisons test for reviewing statistical differences between the biomaterial groups (pNC & Albugel vs pNC & NPgel vs pNC & NPgel/dNCM). When analysing the percentage of pNC positive for a phenotype marker, a Kruskal-Wallis test was performed, followed by Dunn's post hoc test to compare each group (pNC & Albugel vs pNC & NPgel vs pNC & NPgel/dNCM). For the statistical analysis of GAG production data was normally distributed therefore a one-way ANOVA was performed, followed by the recommended Tukey's multiple comparisons test to compare each acellular biomaterials (Albugel vs NPgel vs NPgel/dNCM) and the equivalent cellular construct (Albugel vs pNC & Albugel; NPgel vs pNC & NPgel; NPgel/dNCM vs pNC & NPgel/dNCM). Statistical significance was accepted at $p \leq 0.05$.

Table 1. Immunohistochemical procedures utilised for phenotypic characterisation of porcine notochordal cells.

Primary Antibody	Target	Clonality	Optimal dilution	Antigen retrieval	Technique	Secondary Antibody	Optimal dilution
Aggrecan (Abcam, ab3778)	NP matrix	Mouse monoclonal	1:100	Heat	IHC	Rabbit Anti-Mouse (Abcam, ab6727)	1:500
Brachyury (Abcam, ab20680)	NC/NP marker	Rabbit polyclonal	1:100	None	IHC	Goat Anti-Rabbit (Abcam, ab6720)	1:500
Collagen Type II (Sigma, maB1330)	NP matrix	Mouse monoclonal	1:200	Enzyme	IHC	Rabbit Anti-Mouse (Abcam, ab6727)	1:500
KRT 8/18/19 (Abcam, ab41825)	NC/NP marker	Mouse monoclonal	1:400	Enzyme	IHC	Rabbit Anti-Mouse (Abcam, ab6727)	1:500

Primary antibody target, clonality, dilutions optimised and antigen retrieval. Along with the Secondary antibodies and dilutions, that was used alongside for immunohistochemical staining the staining methods.

Results

Rheological Properties

Storage moduli of the three biomaterials (post-gelation) were monitored over a range of strain values (Fig. 1). During the strain sweep (or amplitude sweep) experiment, all three hydrogels behaved like a viscoelastic solid characterised by a higher storage modulus (G′) than loss modulus (G″). A gradual downturn of G′ can be seen in every sample as the strain value was increased. However, the elastic portion of these materials prevailed the viscous portion throughout the strain range tested here (no G′ and G″ crossover). In both acellular NPgel and acellular NPgel/dNCM systems, the storage moduli increased after 24 hours, reaching an average G′ of ~14 kPa and ~3 kPa (at 1 Hz), respectively. These two hydrogel systems exhibited modest shrinkage (up to 20 % by volume) after 24 hours of media immersion. The slight change in volume was associated with the release of water as a result of interaction with the salts present in the media, creating a denser scaffold with higher G′. Albugel did not display shrinkage during the 24-hour period and maintained a G′ value of ~0.8 kPa at both time points. The strain-independent region of an amplitude sweep, also known as the linear viscoelastic (LVE) region, describes the limits within which a viscoelastic material can be deformed non-destructively. Whilst all three biomaterials displayed linear viscoelastic properties within physiological strain ranges and thus were progressed for further cell testing, the LVE limit of Albugel (up to 40 % strain) exceeded that of NPgel (7 % strain) and NPgel/dNCM (10 % strain) (Fig. 1).

Optimising Cell Seeding Density within NPgel as an Example Biomaterial

An initial optimisation experiment was conducted to determine seeding density and to observe if different cell densities influenced the morphology and survival of pNC *in vitro* following 2 weeks culture within NPgel as the example biomaterial. Cells were visible in the 1×10^6 cells/mL constructs, but they were sparse, and presented as single cells (Fig. 2). Cell clustering was observed in biomaterial constructs seeded with 4×10^6 cells/mL, 1×10^7 cells/mL and 2×10^7 cells/mL. There was no observable difference between the 4×10^6 cells/mL and 1×10^7 cell/mL, and in the constructs seeded at 2×10^7 cells/mL displayed smaller clusters with dispersed single cells (Fig. 2). As clusters were first observed in 4×10^6 cells/mL, further experimental set ups were performed with 4×10^6 cells/mL seeding density in biomaterials.

Isolated Notochordal Cell Morphology in NPgel as a Model Biomaterial

Optimisation experiments were conducted to determine whether pNCs could be maintained within a biomaterial system. Phase contrast images demonstrated the presence of large cell clusters within NPgel, with predominant vacuoles seen up to 2 weeks in culture, which are still visible at 3 weeks (Fig. 3; vacuoles indicated by black arrowheads).

Porcine Notochordal Cells in Albugel, NPgel and NPgel/dNCM

Live-cell imaging with Calcein-AM and Hoechst staining, demonstrated that pNCs remained present and viable up to 2 weeks in all biomaterials. The maintenance of NC morphology and the retention of vacuole-like structures (indicated with white arrows) were observed in the 1-week NPgel and up to 2-week in the Albugel samples seeded with pNCs, although quantification was not possible given the clustered appearance of cells (Fig. 4). NPgel/dNCM with pNC showed less notochordal-like morphological phenotype with no vacuoles present at any timepoints (Fig. 4).

Constructs were further cultured for an extended 4-week culture. Scanning electron microscopy was utilised to investigate morphology of acellular and cellular biomaterials. Furthermore, histological stains: H+E, Alcian Blue, Masson's Trichrome and Safranin O/ Fast green were used to determine the morphology and matrix deposition by the cells in the biomaterials.

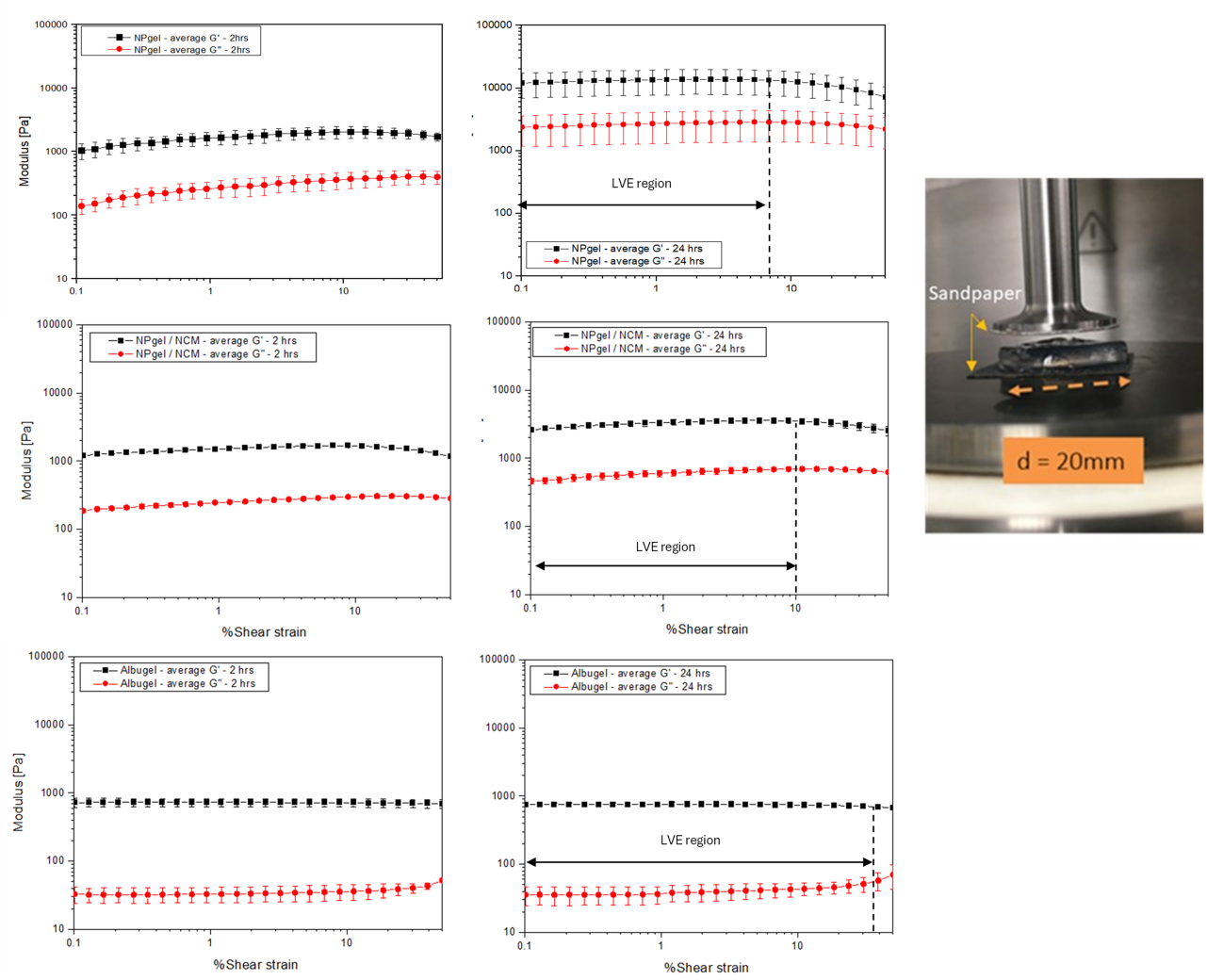

Fig. 1. Storage moduli of the three biomaterials (post-gelation). Amplitude sweeps of the NPgel, NPgel/dNCM and Albugel after 2- and 24-hours immersion in culture media which mimics the degenerate conditions of the disc (OSM, pH, glucose). Experimental setup is shown on the right-hand side.

Scanning Electron Microscopy Morphology

SEM analysis of acellular constructs demonstrated a porous structure within all biomaterials. Albugel demonstrated a dense structure with fibrous pores (Fig. 5**A**). Whilst NPgel displayed a more honeycomb porous structure (Fig. 5**C**), which following inclusion of dNCM showed the appearance of thinner strands (Fig. 5**E**). Whilst constructs containing pNCs demonstrated apparent cellular structures within all gel systems (Fig. 5). Although constructs were heterogeneous, with some areas filled with cellular structures, other areas were devoid of cells (Fig. 5**B,D,E**), suggesting an uneven distribution of pNCs within the constructs. The majority of cells within all three biomaterials were seen in small clusters (Fig. 5**B,D,E**), although some single/duplicate cells were observed in Albugel constructs (Fig. 5**Biii**). Within NPgel constructs some clusters displayed a visible 'membrane' which appeared to wrap the entire pNC cluster (Fig. 5**D**; white arrowheads).

Isolated Notochordal Cell Behaviour and Morphology in Novel Biomaterials

H+E staining of pNC & NPgel and pNC & NPgel/dNCM demonstrated the seeded cells remained in cluster formation, whereas the pNCs in the Albugel construct appeared more dispersed (Fig. 6). Alcian Blue demonstrated GAG staining around the cell clusters (stained blue) in pNC & NPgel constructs (Fig. 6). In the NPgel and NPgel/dNCM constructs (Fig. 6) Masson's Trichrome blue staining surrounding the cells indicates collagen expression in the surrounding material (Fig. 6). Collagen expression is also indicated in Safranin Orange stain by pericellular green/turquoise staining (Fig. 6). Albugel constructs failed to demonstrate clear matrix indication when stained with Alcian Blue or Masson's Trichrome, however Safranin Orange stain indicated slight green/turquoise staining surrounding the pNC (Fig. 6).

The number of cells per cluster was determined fol-

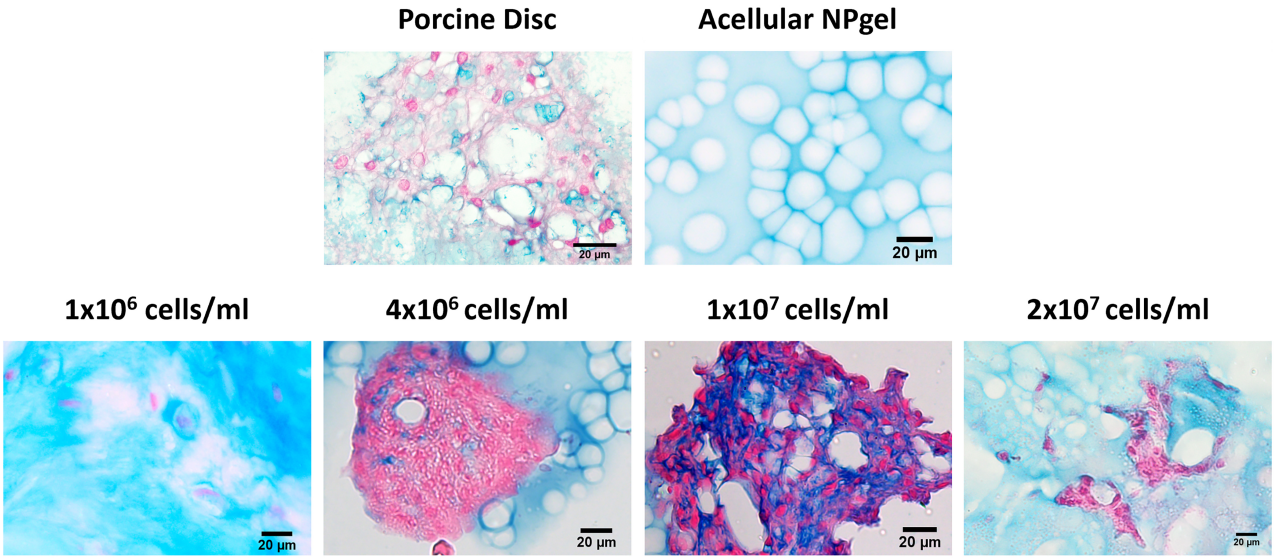

Fig. 2. Optimised seeding density of cells into biomaterials. Porcine notochordal cells seeded at different densities; 1×10^6, 4×10^6, 1×10^7, and 2×10^7 before culturing for up to 2 weeks in 5 % v/v oxygen and stained with alcian blue. Scale bar 20 µm.

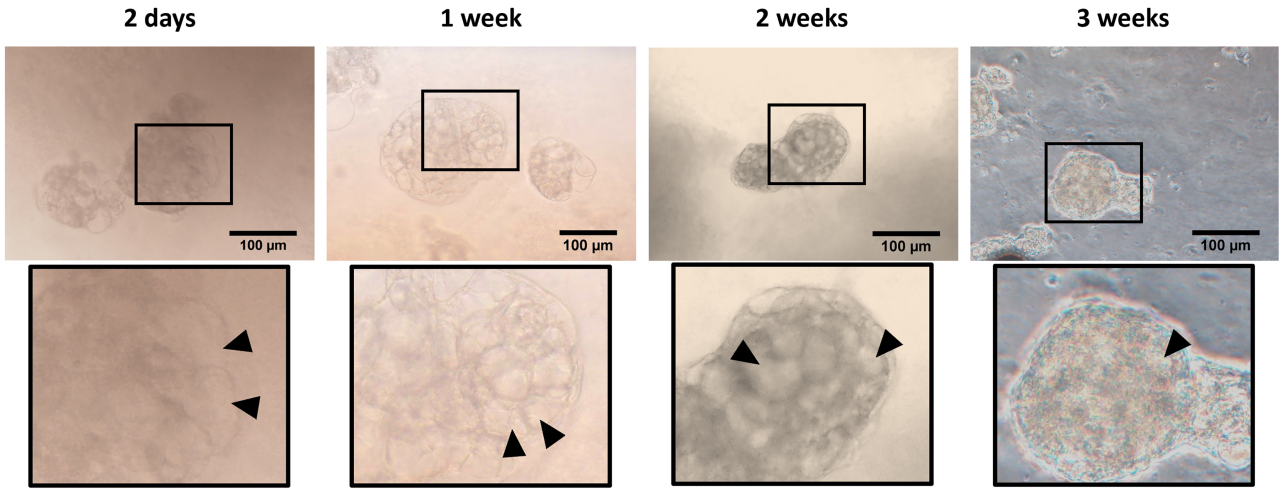

Fig. 3. Brightfield live cell imaging of porcine notochordal cells cultured in NPgel, for up to 3 weeks in a hypoxia unit of 5 % v/v oxygen at 37 °C. Scale bar 100 µm. Black arrowheads indicate vacuoles.

lowing 4 weeks in culture. The number of cells in clusters were significantly different between each biomaterial, with the number of pNCs in clusters when cultured in NPgel, were significant greater when compared to NPgel/dNCM ($p \leq 0.01$) and significantly greater when compared to Albugel ($p \leq 0.0001$); NPgel/dNCM were significantly greater when compared to Albugel ($p \leq 0.001$; Fig. 7). With the highest number of cells observed per cluster of 40 cells in NPgel, 26 in NPgel/dNCM and 14 cells in Albugel, with the median number of cells observed per cluster was 5 in NPgel, 2 in NPgel/dNCM and 1 in Albugel (Fig. 7). Altogether, this demonstrated that pNCs present themselves in larger clusters in NPgel and NPgel/dNCM biomaterials, whereas in Albugel they were mostly single cells.

Notochordal Cell Characterisation and Phenotypic Analysis within Novel Biomaterials

Immunohistochemical staining was further used to analyse and characterise the pNC that were cultured in the biomaterials for 4 weeks (Fig. 8**A**). The pNCs seeded into all three biomaterials showed nuclear and cytoplasmic positive staining for the NC/NP cell markers brachyury and cytokeratin 8/18/19, which when quantified showed no significant difference in expression between the biomaterials ($p > 0.05$) (Fig. 8**B**). Extracellular immunohistochemical staining for aggrecan was shown in the pNCs seeded into Albugel, NPgel and NPgel/dNCM, with extracellular immunohistochemical staining for collagen type II only distinguishable in the pNC & NPgel constructs (Fig. 9). How-

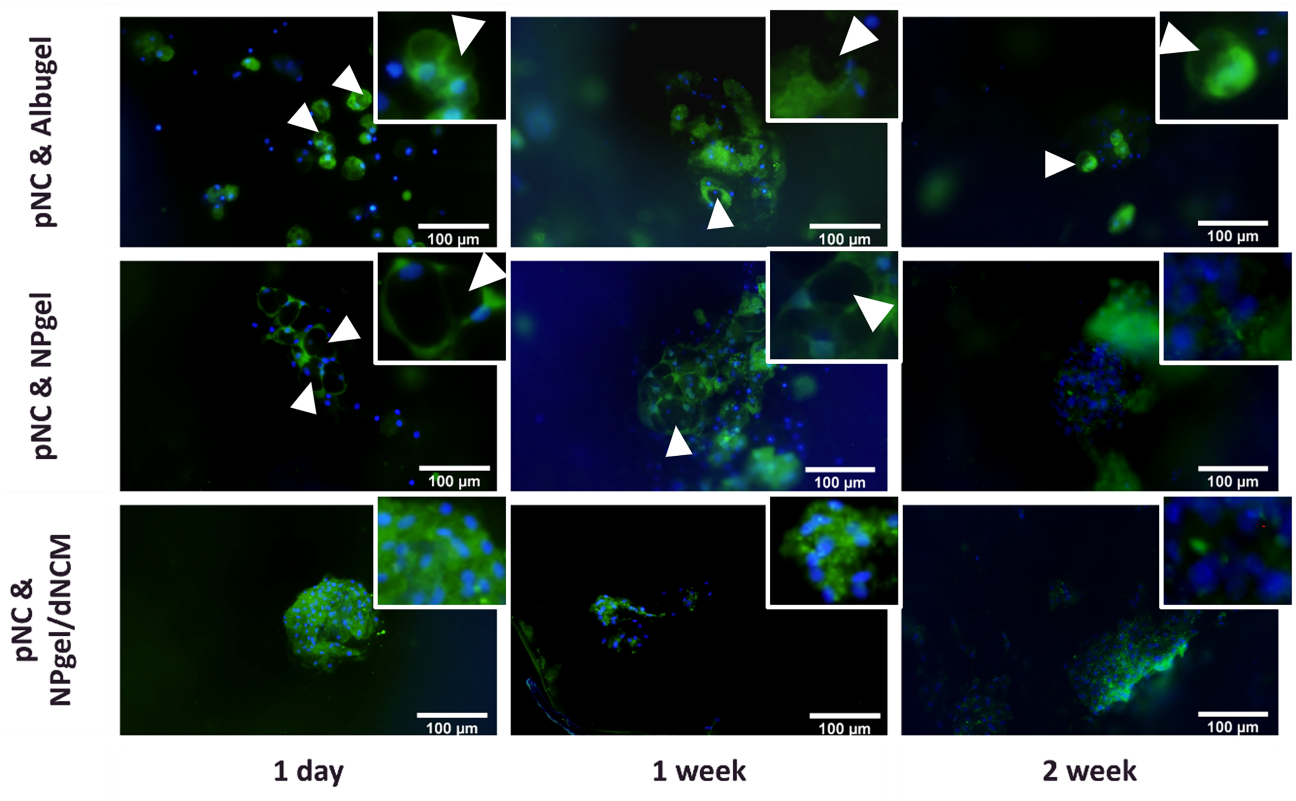

Fig. 4. Immunofluorescence staining of live cell imaging of porcine notochordal cells cultured in NPgel, NPgel/dNCM and Albugel, for up to 2 weeks in a hypoxia unit of 5 % v/v oxygen. Images were captured using Calcein-AM and Hoechst 33342. White arrowheads indicate vacuoles.

ever, staining was also observed in the acellular NPgel and NPgel/dNCM construct, due to the nature of biomaterials retaining DAB (Fig. 9).

GAGs released into the culture media from pNC and biomaterial constructs was assessed throughout the 4-week culture period and analysed using DMMB assay (Fig. 10). The acellular NPgel/dNCM constructs had a significantly higher GAG release into the culture media compared to acellular NPgel and Albugel biomaterials at 1 week (NPgel/dNCM vs Albugel, $p \leq 0.001$; NPgel/dNCM vs NPgel, $p \leq 0.001$), 2 week (NPgel/dNCM vs Albugel, $p \leq 0.0001$; NPgel/dNCM vs NPgel, $p \leq 0.01$) and 3-week (NPgel/dNCM vs Albugel, $p \leq 0.01$; NPgel/dNCM vs NPgel, $p \leq 0.01$) culture time points but was reduced following 4 weeks in culture ($p > 0.05$). This may suggest release of the natural GAGs coming from the dNCM within the biomaterial, with no further increase of GAG release into media within NPgel/dNCM materials seeded with pNCs. No significant difference in GAG release was observed between acellular controls and pNC-containing constructs at any time-point (Fig. 10).

Discussion

NCs have attracted considerable interest due to their potential application for regeneration of the intervertebral disc (Bach *et al.*, 2022), but to date, to the authors knowledge only one study investigated the potential of one biomaterial to support their viability and matrix production with limited phenotypic investigations made, with studies mainly investigating simple 3D culture systems to maintain phenotype for *in vitro* applications.

This study investigated three potential biomaterials which are all injectable and could provide potential mechanical support to the IVD whilst delivering the regenerative cell source. The selected biomaterials represented a naturally inspired cross linked hydrogel (Albugel), a fully synthetic hydrogel which gels based on entanglement of polymer chains (NPgel) (Boyes *et al.*, 2021), and the supplementation of the synthetic hydrogel with naturally derived dNCM (NPgel/dNCM) (Schmitz *et al.*, 2022). All three acellular biomaterials demonstrated viscoelastic stability within the physiological strain range observed for IVDs. NPgel exhibited a higher gel strength (characterised here by G′) compared to NPgel/dNCM and Albugel. Furthermore, NPgel and to a lesser extent NPgel/dNCM showed an increase in G′ following 24 hrs in culture media which mimics the degenerate IVD. The G′ of NPgel following 24 hrs in degenerate media reached ~14 KPa which is similar to that of human NP tissue reported previously of 7-21 kPa (Iatridis *et al.*, 1997; Iatridis *et al.*, 1996). We have previously reported other rheological properties of NPgel

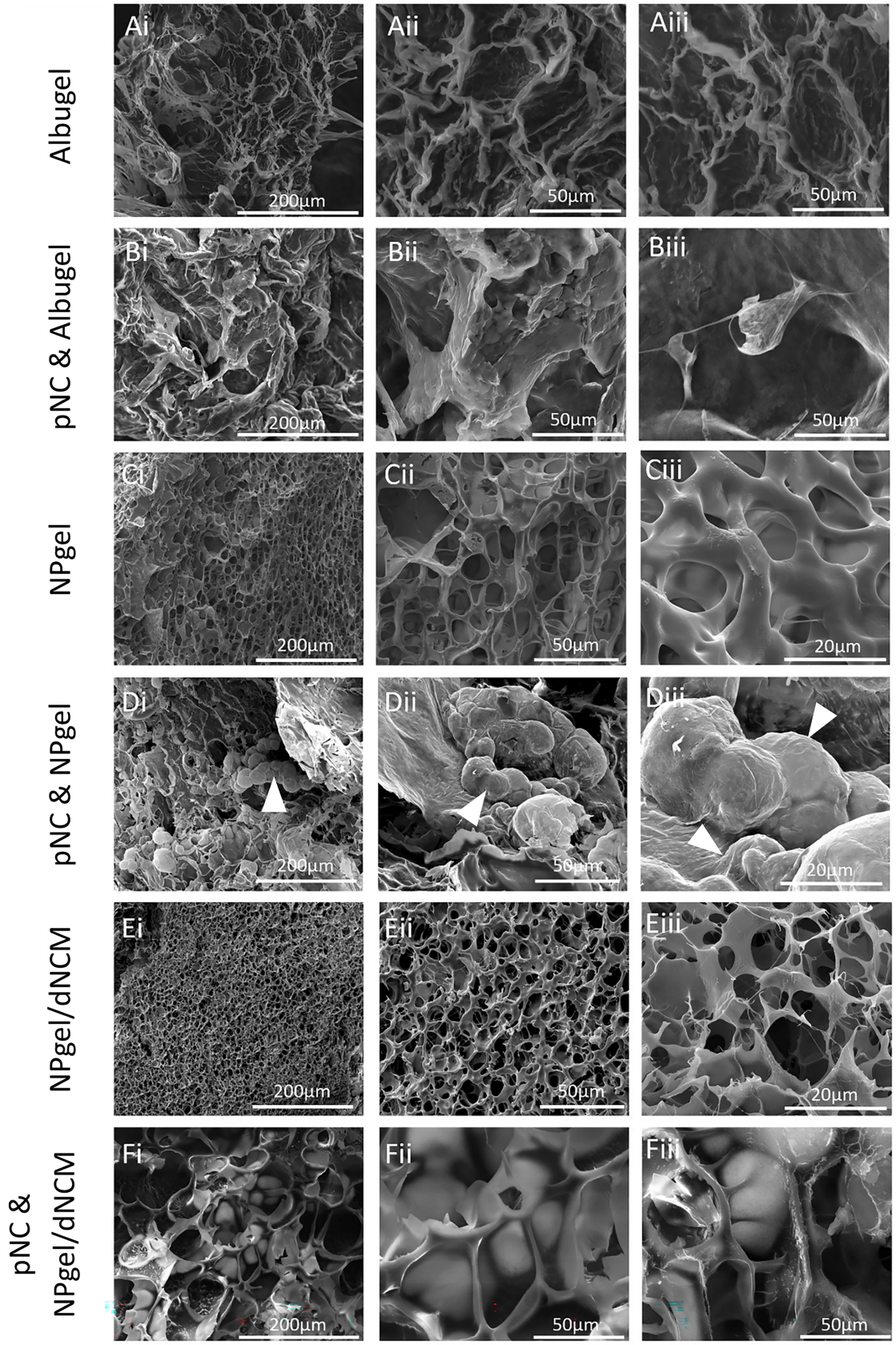

Fig. 5. Scanning electron microscope images acellular biomaterials and those containing porcine notochordal cells (pNC), cultured for 2 weeks in a hypoxia unit of 5 % oxygen at 37 °C. (**A**) Acellular Albugel; (**B**) pNC cultured in Albugel; (**C**) Acellular NPgel; (**D**) pNCs cultured in NPgel; (**E**) Acellular NPgel/dNCM; (**F**) pNCs cultured in NPgel/dNCM. White arrow heads indicate where a visible 'membrane' which appeared to wrap the entire pNC cluster was seen. Scale bars as indicated (20, 50 or 200 µm).

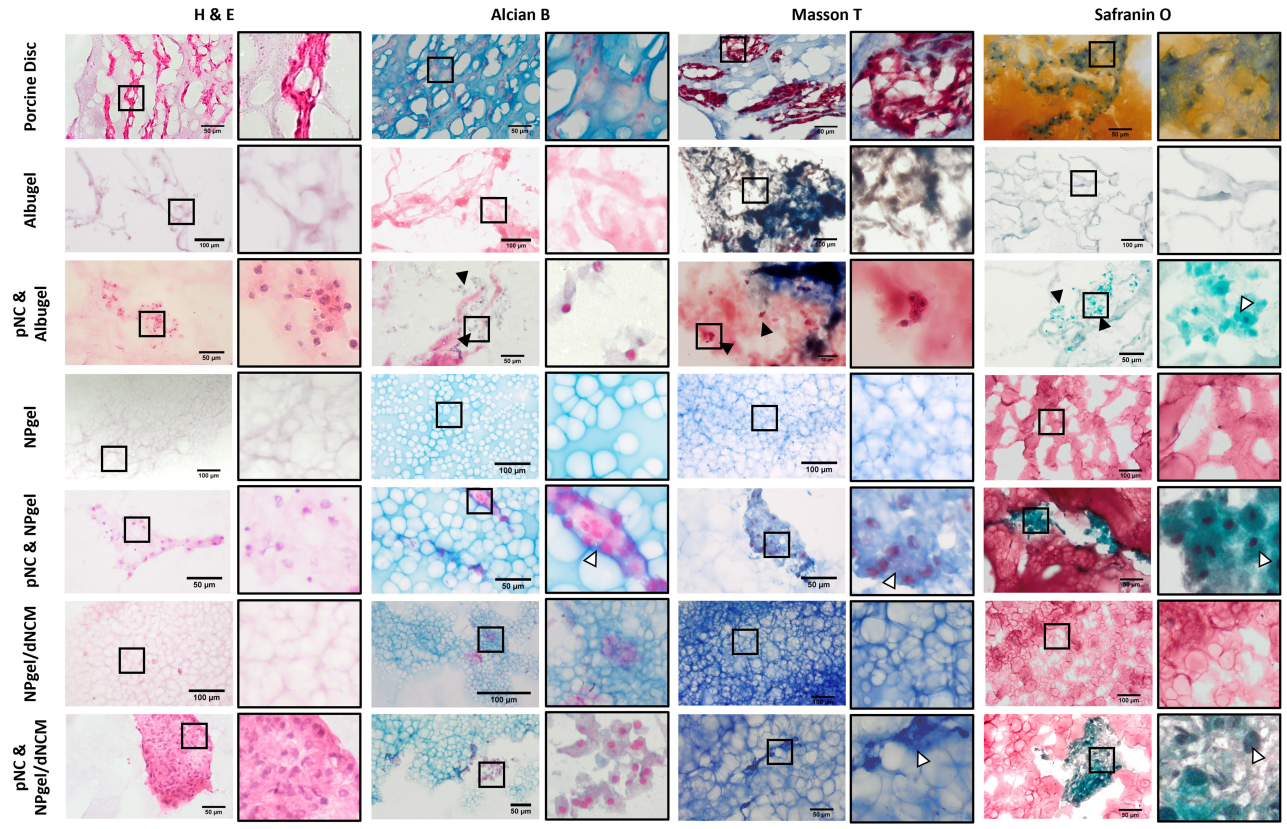

Fig. 6. Porcine notochordal cell (pNC) morphology when cultured in Albugel (pNC & Albugel), NPgel (pNC & NPgel) and NPgel/dNCM (pNC & NPgel/dNCM) with acellular controls (Albugel; NPgel; NPgel/dNCM), for up to 4 weeks in 5 % oxygen. Haematoxylin and Eosin (H+E), Alcian Blue (Alcian B), Masson's Trichrome (Masson T) and Safranin Orange (Safran O). Black arrows highlight where cells are present. Images with black outline are high magnification regions of cellular constructs, white arrows indicate extracellular matrix deposition. Porcine disc and cellular constructs are scale bar 50 µm, acellular constructs scale bar 100 µm.

including its gelation kinetics (Boyes *et al.*, 2021). Initial studies with pNCs utilised NPgel to determine the seeding density for future studies. Porcine NCs were seeded at different cell densities ranging between 1×10^6 cells/mL to 2×10^7 cells/mL into NPgel, where pNCs presented mainly in clusters and easier to identify within sectioned materials at 4×10^6 cells/mL and 1×10^7 cells/mL. Whilst lower densities of 1×10^6 cells/mL displayed mainly single cells and the highest cell density of 2×10^7 cells/mL displayed both clustered and single cells but showed no advantage over lower seeding densities. The native cell density of the NP has been reported to be 1.3×10^5 cells/cm^3 in non-chondrodystrophic dogs (Hunter *et al.*, 2003), and 4×10^6 cells/cm^3 in humans (Maroudas *et al.*, 1975). The importance of preservation the pNC clusters phenotype was also hypothesised to support NC survival and function (Aguiar *et al.*, 1999; Gantenbein *et al.*, 2014; Humphreys *et al.*, 2018; Hunter *et al.*, 2003; Spillekom *et al.*, 2014). Additional, NCs are also reported to be highly metabolically active and sensitive to nutrient deprivation (Guehring *et al.*, 2009; Spillekom *et al.*, 2014), therefore the optimum cell density was selected as 4×10^6 cells/mL, as cluster formation was retained without excessive cell density which could provide nutrient deprivation over long term culture and is also in agreement with the cell density reported in human NP (Maroudas *et al.*, 1975; Roughley, 2004). Based on brightfield images pNCs showed clear cluster and vacuole structures up to at least 2 weeks in culture, thus following these successful initial results, the complete screening experiment was performed, seeding pNC into three biomaterials that have shown potential for disc regeneration.

Retention of Notochordal Cell Cytomophology in Biomaterials

From the histological images, it was promising to observe that pNCs survived for up to 4 weeks in all three biomaterials, however the morphotypic pNC was not retained in all biomaterials. In Albugel, Calcein-AM images, SEM and histology, showed a lack of large clusters, with most cells observed in single cells. However, some preservation of vacuole-like structures was observed after 2-weeks and key NC/NP markers were retained, including brachyury and keratin 8/18/19. In native NP tissue, single cells are usually smaller and resemble more the mature NP cells often seen in a more mature and degenerate disc (Chen *et al.*, 2006; Hunter *et al.*, 2003), suggesting

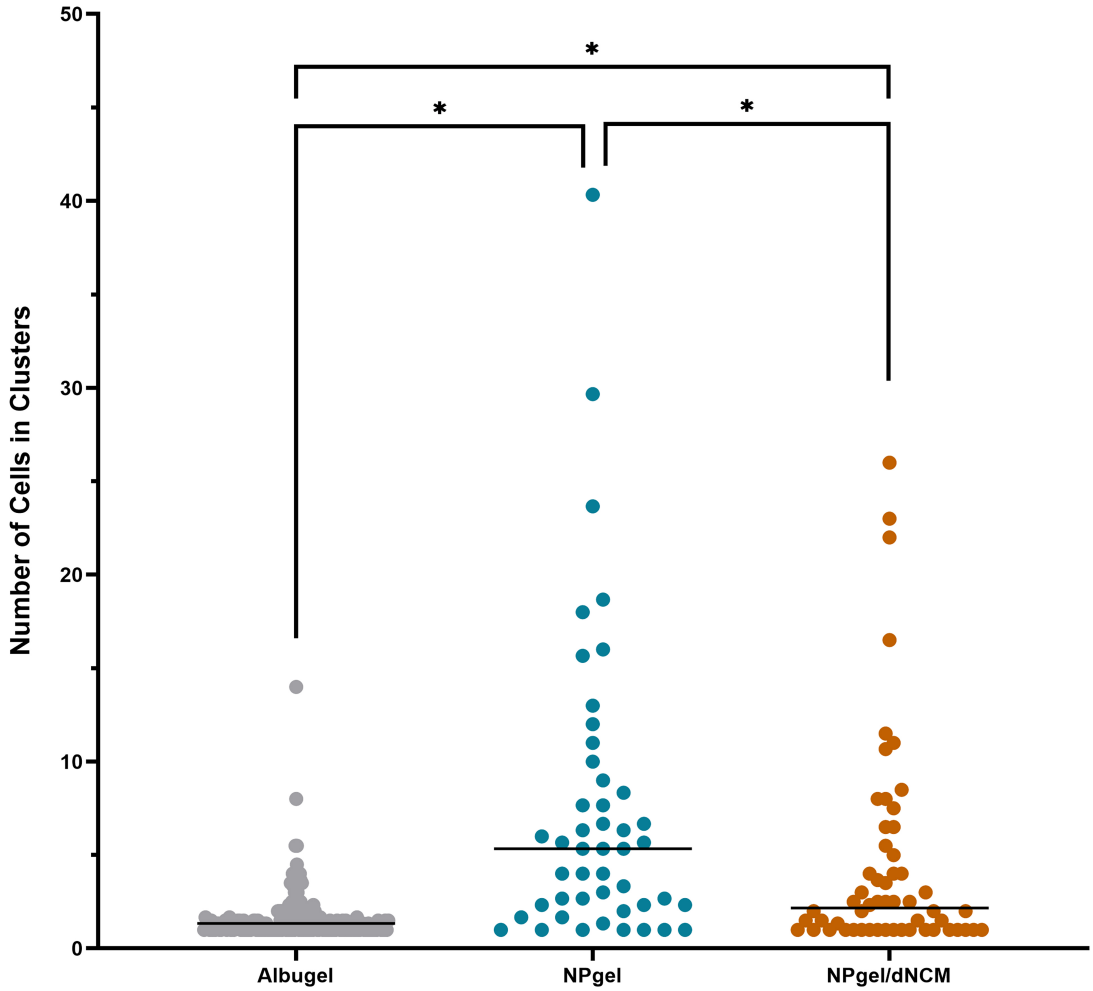

Fig. 7. Porcine notochordal cell (pNC) cluster size when seeded into biomaterials; NPgel, NPgel/dNCM and Albugel after 4 weeks in culture at 5 % v/v oxygen. A single dot represents a cluster of pNCs. * $p \leq 0.05$.

that the pNC in Albugel were differentiating into these mature NP cells. Within the literature their remains some debate to whether the population of smaller mature NP cells are derived from the juvenile NCs or replaced from alternative progenitor cells (Kim *et al.*, 2009), whereas these results support the perspective that NCs have the capability to differentiate into mature NP cells, which can retain their expression of brachyury and cytokeratin (Minogue *et al.*, 2010; Risbud *et al.*, 2010). In NPgel, the pNCs predominately presented in clusters and contained vacuolated structures evident in Calcein-AM stained live-cell images, within this biomaterial clusters containing up to 40 cells per cluster were maintained. However, following long term culture of 4-weeks the vacuole-like phenotype was lost despite the pNC remaining in clusters. Similar findings were also observed during a longer-term culture of NCs in alginate beads, despite the maintenance of phenotypic markers, the morphology of the cells changed from large NC clusters to NCs with smaller vacuoles and mature NP cells (Arkesteijn *et al.*, 2015). The loss of vacuole morphology along with loss of phenotypic markers was also noted when NC were cultured in monolayer (Arkesteijn *et al.*, 2015) and when injected directly into NP tissue (Arkesteijn *et al.*, 2017). In NPgel/dNCM, histological images, SEM and cell cluster size analysis demonstrated the presence of clusters and vacuole like structures were observed, although this was not visualised within live-cell imaging. A study by Ma *et al.* (2013) utilised rabbit NCs seeded in a link-N self-assembling peptide scaffold, demonstrating that rabbit NCs viability was maintained and could deposit aggrecan and type II collagen after 14 days of 3D culture and reported the presence of phenotypic vacuoles at 7 days of 3D culture but did not study further their phenotype using other phenotypic markers.

Retention of Notochordal Cell Phenotype in Biomaterials

The histological and IHC images demonstrated the indication of pericellular matrix deposition containing aggrecan staining observed in the pNC & Albugel, pNC & NPgel and pNC & NPgel/dNCM constructs, which also cor-

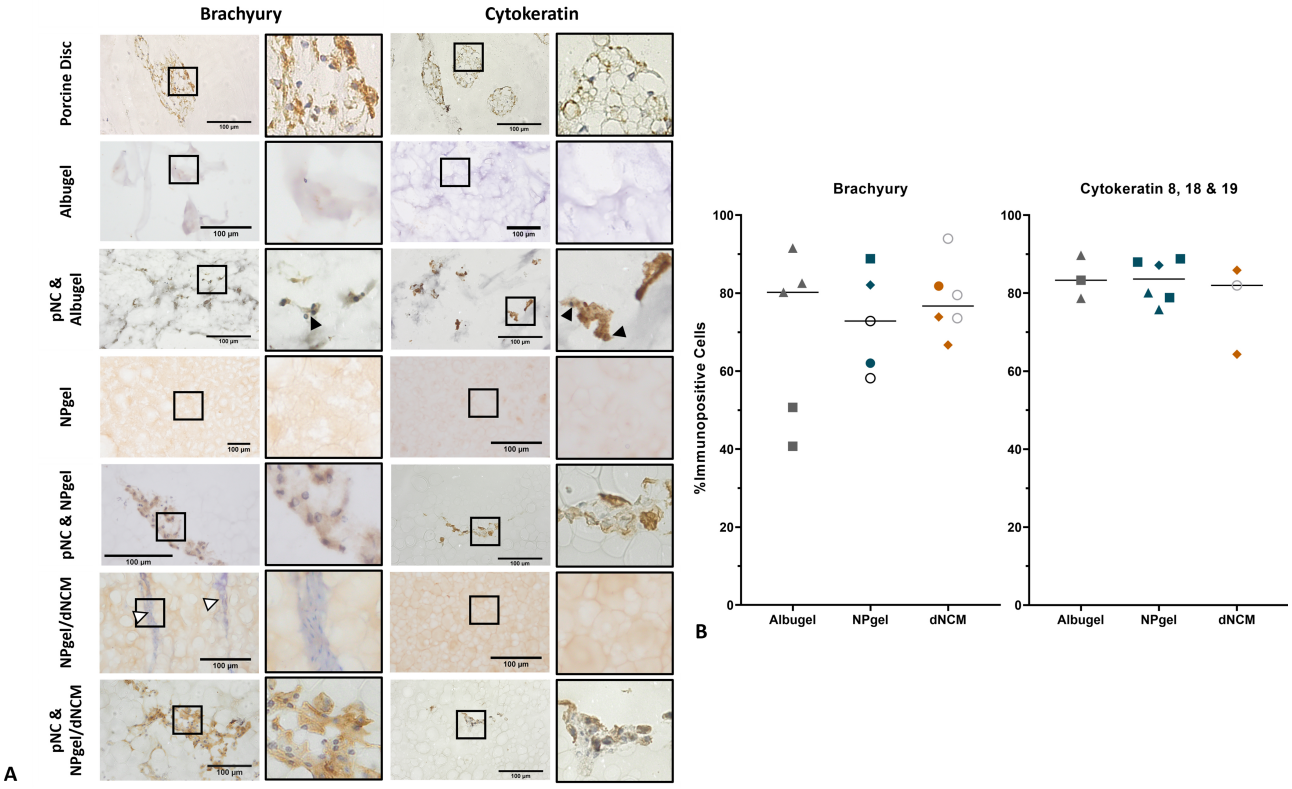

Fig. 8. Porcine notochordal cell phenotype when cultured in three biomaterials. (**A**) Immunohistochemistry staining of porcine notochordal cells (pNC) seeded in biomaterials Albugel (pNC & Albugel), NPgel (pNC & NPgel) and NPgel/dNCM (pNC & NPgel/dNCM) and cultured for up to 4 weeks in 5 % v/v oxygen at 37 °C, including acellular controls (Albugel; NPgel; NPgel/dNCM) and porcine disc. Stained with Brachyury, Cytokeratin 8/18/19 (pan Cytokeratin). Black boxed images represent zoomed in images of pNC in biomaterials and porcine disc. Black arrows highlight pNC. White arrows highlight residual cellular staining from dNCM. Scale bar 100 µm. (**B**) Quantitative analysis of the percentage of Brachyury and cytokeratin 8/18/19 immunopositive cells in pNC & Albugel (Albugel), pNC & NPgel (NPgel) and pNC & NPgel/dNCM (NPgel/dNCM). Each shape represents a different biological repeat.

responded to the turquoise GAG stain within Alcian Blue (Leung *et al.*, 2009). Interestingly, collagen type II staining was only strongly observed in pNC cultured within NPgel. IHC demonstrated the retention of brachyury and cytokeratin NC/NP phenotypic markers. Studies using NCs in alginate beads have also shown cell survival during culture, which corresponded with brachyury and cytokeratin expression and an increase in GAG detection (Aguiar *et al.*, 1999; Arkesteijn *et al.*, 2017; Gantenbein-Ritter & Chan, 2012). Within the current study there was limited GAG release evidenced from pNCs cultured within the biomaterials, with only Albugel demonstrating a difference between acellular and cellular constructs. Potentially suggesting the hyaluronic acid within the Albugel increases GAG production. Alternatively, the lack of GAG release into the media in NPgel constructs could indicate greater GAG retention in the NPgel constructs containing pNCs, as histological staining did display cellular GAG staining using both Alcian Blue and Safranin O. Whilst NPgel supplemented with dNCM demonstrated high secretion of GAGs into the media even in acellular controls over the first 3 weeks, this decreased after 4 weeks in culture. Suggesting loss of the dNCM (which is GAG rich) into the media over the initial time course. The decreased GAG content in the media after 4 weeks may indicate exhaustion of the GAG content from the dNCM or potentially the formation of a more complex matrix network leading to the trapping of the GAGs at later time course. However, given the low collagen staining observed with Masson's Trichrome staining and immunohistochemical staining for collagen type II it is more likely the dNCM had leached out over the first 3 weeks. The incorporation of dNCM into NPgel is based on a physical entanglement rather than any physical cross linkages and thus it may be necessary to develop biomaterials which enable chemical cross linking of NCM into the materials to ensure longer term retention. Additionally, in Ma *et al.* (2013) a Link-N self-assembled scaffold biomaterial promoted the accumulation of aggrecan and collagen type II when seeded with rabbit NCs (Ma *et al.*, 2013). Furthermore, when such a system is injected into the NP tissue space in a whole IVD the GAG release would likely be retained in the disc and thus this leaching out may not be a detriment follow-

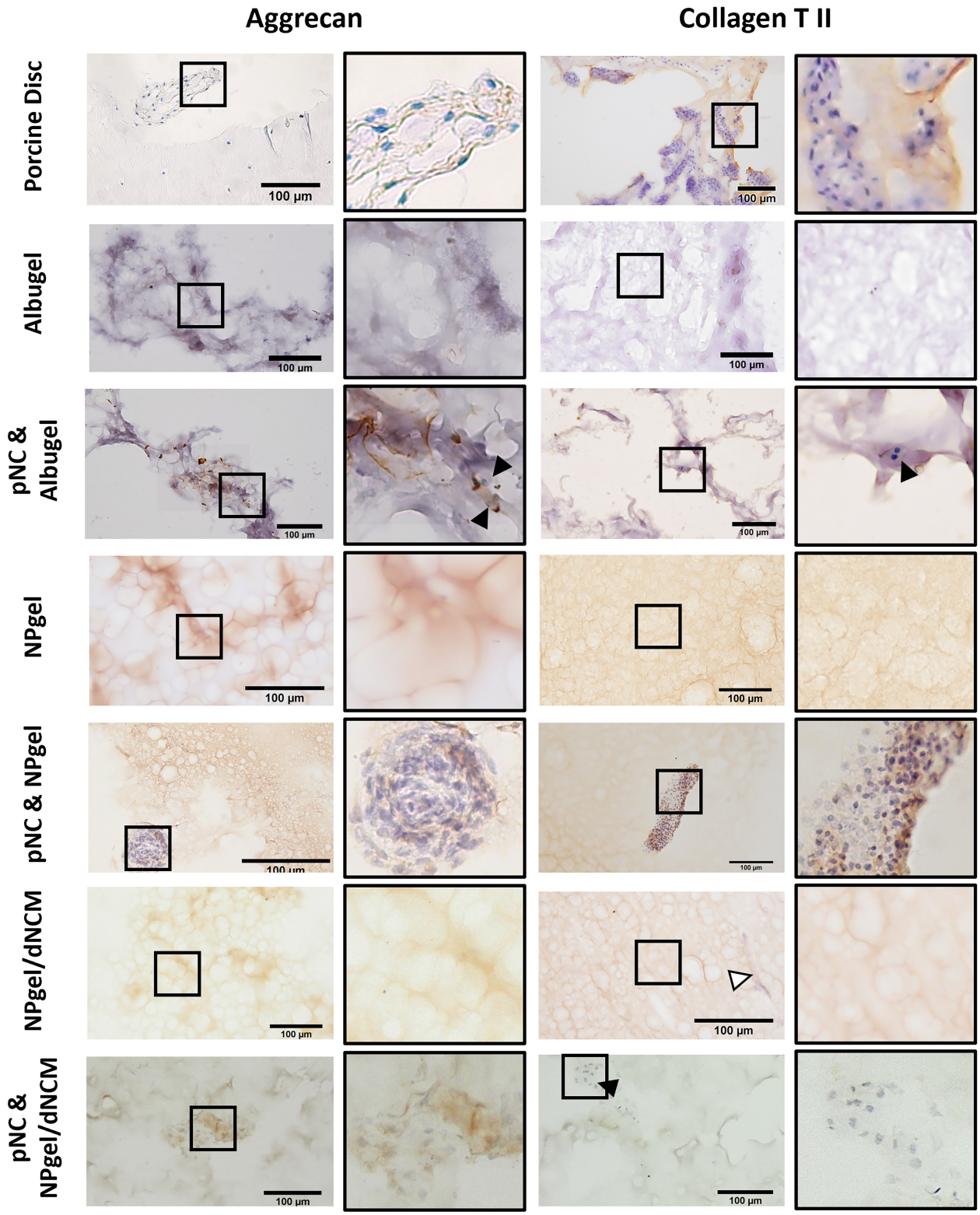

Fig. 9. Porcine notochordal cell (pNC) extracellular matrix expression when seeded in biomaterials. Immunohistochemistry staining of pNCs seeded in biomaterials Albugel (pNC & Albugel), NPgel (pNC & NPgel) and NPgel/dNCM (pNC & NPgel/dNCM) and cultured for up to 4 weeks in 5 % v/v oxygen at 37 °C, including acellular controls (Albugel; NPgel; NPgel/dNCM) and porcine disc. Stained with Aggrecan and Collagen type II (Collagen T II). Black boxed images represent zoomed in images of pNC in biomaterials and porcine disc. Black arrows highlight pNC. White arrows highlight residual cellular staining from dNCM. Scale bar 100 µm.

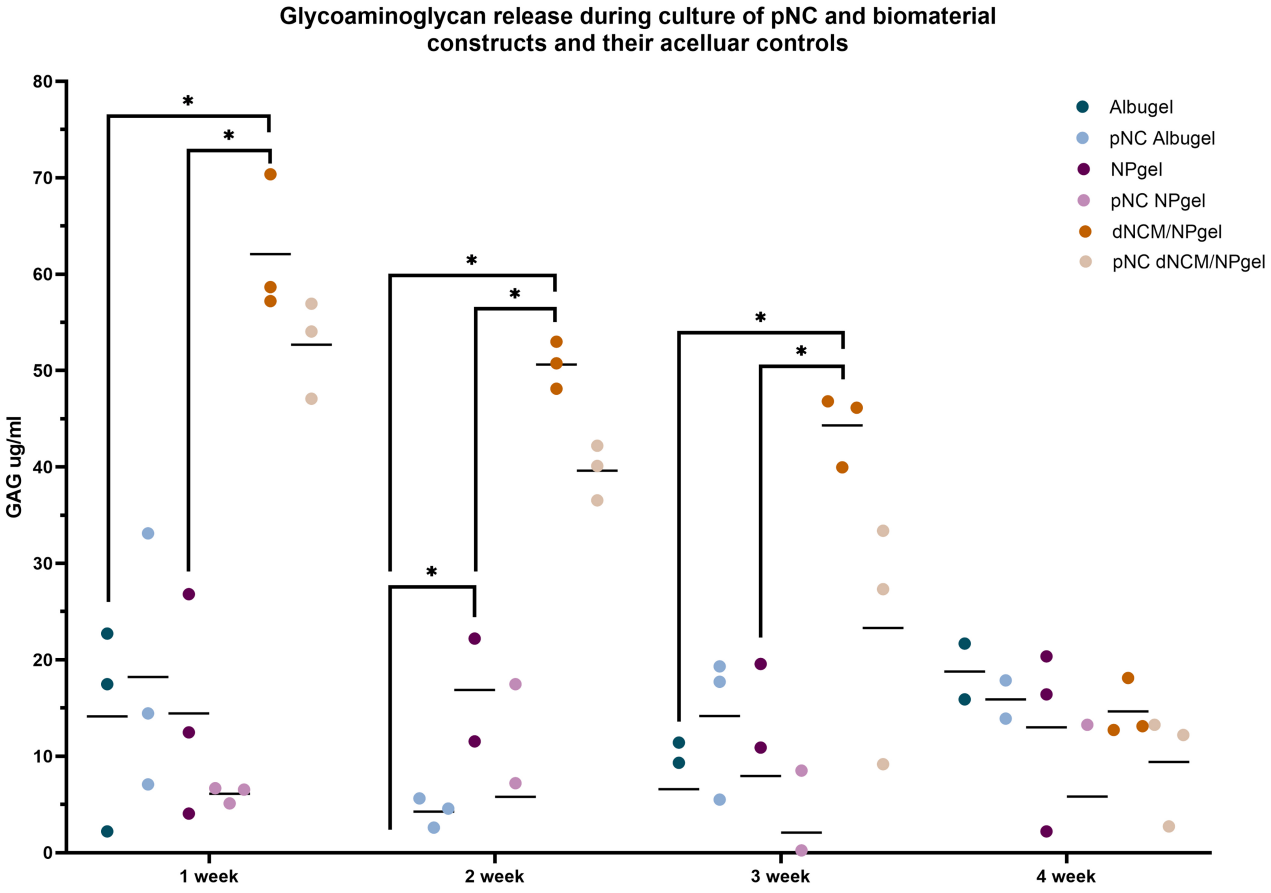

Fig. 10. Porcine notochordal cell glycosaminoglycan (GAG) release during culture in biomaterials. GAG release was measured using 1,9-Dimethylene blue (DMMB) assay in media collected over 4 weeks of acellular biomaterials (Albugel, NPgel and NPgel/dNCM) and porcine notochordal cells (pNC) seeded in Albugel, NPgel and NPgel/dNCM biomaterials at 4 × 10^6 cells/mL and cultured at 5 % v/v oxygen at 37 °C for up to 4 weeks. *$p \leq 0.05$.

ing IVD injection. Alternative methods of assessing extracellular matrix production by the seeded cells, such as the use of tagging cellular GAG production as used by Baskin *et al.* (2007) would enable a better understanding whether the observed matrix staining was produced from the pNCs themselves rather than a remnant from the biomaterial.

Vacuoles within Cultured Notochordal Cells

The seeding of pNC in the three biomaterials resulted in the presentation of morphologically different cells, which was characterised by the gradual loss of vacuoles, but a retention of NC cell marker expression. The purpose of NC vacuolation in embryonic development of the spine is focused on retaining hypertonic tension (Hunter *et al.*, 2007). Taking NCs into an *in vitro* setting does have the limitation of altering the cells environment; in this study the constructs were maintained in physiologically relevant hypoxic conditions of 5 % oxygen (Chen *et al.*, 2014; Soukane *et al.*, 2005), and using media recommended for IVD 3D culture (Basatvat *et al.*, 2023). Nevertheless, with the isolation of cells, there is a change of environment such as the loss of mechanical stress and extracellular matrix which otherwise would have promoted water retention, although by maintaining cell clusters the pericellular matrix should be retained (Oegema, 1993; Urban *et al.*, 1978). All three biomaterial systems investigated here are hydrogel-based biomaterials, which have high water-soluble polymeric materials. In the biomaterial that contains NC matrix, (NPgel/dNCM), there was some evidence of the retention of vacuole-like structures. In previous studies where altered media osmolarity has been tested, from standard 300 to 500 mOsm/L this resulted in a sustained canine NPC population with improved phenotype, irrespective of oxygen conditions (Laagland *et al.*, 2022; Spillekom *et al.*, 2014), suggesting that there could be many factors that can affect the NC phenotype. It may be that the lack of external mechanical and hydrostatic tension caused the difference in NC morphology, as vacuoles function to withstand compression forces (Bagwell *et al.*, 2020; Ellis *et al.*, 2013; Hong *et al.*, 2018; Wang *et al.*, 2017). Although compression loading has also been shown to be detrimental to NC health (Guehring *et al.*, 2010; Hong *et al.*, 2018; Spillekom

et al., 2014; Yurube *et al.*, 2014), whilst other studies have shown no effect on NC viability and phenotype (Saggese *et al.*, 2020). Thus, it would be important to investigate if these pNC seeded biomaterial constructs subjected to physiological compression and loading, would affect morphological NC and their phenotype.

Future Directions

This study was conducted within an *in vitro* setting, to test the potential of biomaterials to retain NC phenotype, as potential delivery systems for regenerative strategies. Such systems will need to be further tested within conditions which mimic more closely the degenerative environment of the disc, such as presence of catabolic cytokines especially IL-1β (Phillips *et al.*, 2015). Furthermore, other features of the degenerate IVD include low glucose which was mimicked in these studies, however low glucose is also accompanied by low pH, the effects of which remain to be determined. If these cell-seeded biomaterials were to become clinically translated as an injectable treatment for disc regeneration, the next phase of testing would be to determine whether the cells could be maintained within a degenerative disc micro-environment. Such a study would need to investigate the complex mico-environment, beyond simply investigating physioxia and low glucose, as investigated in this study. Future testing should also involve analysing mechanical properties of the whole cell-biomaterial construct *ex vivo*, through applying a physiological loading regime (e.g., simulated daily loading). An example of this type of regime would be described as dynamic loading in a human physiological range of between 0.2-1 Mpa disc pressure at 1 Hz (Korecki *et al.*, 2008; Korecki *et al.*, 2010; Chan *et al.*, 2011; Wilke *et al.*, 1999) and may involve a complex loading regime similar to that reported in Le Maitre *et al.* (2009), such studies will provide a more through understanding of the mechanical stability of the materials in combination with cells within a physiologically relevant environment.

Translational Potential

We report here excellent cytocompatibility of the biomaterials screened and provide an insight on how the biomaterials will perform with NCs. If the cell-seeded biomaterial is to be used in a clinical setting as a novel injectable therapy for disc regeneration, it would be regulated as an advanced medicinal product (ATMP). The up-scaling of a product to clinic involves attaining predictable robustness, batch-to-batch variability, safety profiling, reproducibility, and proficiency. Up-scaling the NC-based therapy co-delivered with the seeded biomaterial would involve generating a working cell bank and the involvement of allogeneic cells not only being a far better 'off-the-shelf' business model but a necessity since the human species lose their phenotypic NCs in childhood. As such the options for NC sources include fetal/baby human NCs which comes with significant ethical challenges and are limited in supply. Alternatively, the used of primary xenographic cells from pigs is a possibility, such an approach is growing in clinic applications, as safety is improving with the use of cross-species cells (Sachs, 1994). Based on the successful use of porcine islets cells transplantation in a primate diabetes model in clinical trials, which is accomplished by knocking down the gene for alpha-1,3-galactosyltransferase lacking alpha 1,3-gal sugars on the porcine cell surfaces, that reacts to the innate immune system (Lai & Prather, 2002; Kuwaki *et al.*, 2005; Thompson *et al.*, 2011; Shin *et al.*, 2015).

Conclusions

Three biomaterials, Albugel, NPgel and NPgel/dNCM representing differing classes of natural (Albugel), synthetic (NPgel), and semi-synthetic (NPgel/dNCM) biomaterials were investigated, to determine if they would maintain pNCs phenotype as a first stage to develop a biomaterial delivery system for the IVD. The results determined that pNC can retain viability and maintain NC cell markers in biomaterials, Albugel, NPgel and NPgel/dNCM for up to 4 weeks in physiological 5 % v/v oxygen, however loss of clustering was observed within Albugel and loss of the morphotypic vacuolated NC phenotype was lost or decreased in all three biomaterials. Therefore, the biomaterials selected have the potential to harness NC regenerative properties, however future work is needed to determine whether retention of the morphotypic phenotype is required to provide regenerative properties and mechanical testing of biomaterials following cell cultures is required to understand the true biomechanical stability following application.

List of Abbreviations

ABC, avidin-biotin-complex; FITC, fluorescein isothiocyanate; AF, annulus fibrosus; Albugel, polyethylene glycol-crosslinked serum albumin/hyaluronan hydrogel; ATMP, advanced medicinal product; CLBP, chronic low back pain; DAB, 3,3-diaminobenzidine tetrahydrochloride; DAPI, 4′,6-diamidino-2-phenylindole; DMEM, Dulbecco's modified eagles media; DMMB, Dimethylmethylene blue; dNCM, decellularized NC-matrix powder; FITC, fluorescein isothiocyanate; GAG, glycosaminoglycan; G′, storage modulus; G″, loss modulus; HA, hyaluronic acid; H&E, Haematoxylin & Eosin; IHC, Immunohistochemistry; ITS, Insulin-transferrin-Selenium; IVD, intervertebral disc; LBP, low back pain; LVE, linear viscoelastic; OD, Optical density; MA-HSA, maleimido-human serum albumin; NC, notochordal cells; NP, nucleus pulposus; NPgel, synthetic Laponite® crosslinked poly N-isopropylacrylamide-co-N, N-dimethylacrylamide biomaterial; P/S, Penicillin-Streptomycin; pNC, porcine notochordal cells; PTFE, Polytetrafluoroethylene; SEM, scanning electron microscopy; α-MEM, alpha Minimum Essential Medium.

Acknowledgements

Not applicable.

Author Contributions

RJW, CLM, JS and MT contributed to conception and design of the study; RJW, JS, RJ, TS and SB contributed to acquisition of laboratory data; RJW performed most of the data analysis; RJW, CLM, JS, KB, MT, CS, KI, TS contributed to interpretation of the data; RJW, CLM and JS drafted the manuscript. All authors critically revised the manuscript for intellectual content. All authors approve the final version and agree to be accountable for all aspects of the work.

Ethics Approval and Consent to Participate

All of the tissues used for these studies are from abattoir, no human participants used in this study. Sheffield considers obtaining cadaveric tissue to be exempt from IACUC (animal) and IRB (human) approval.

Funding

This work was supported by the funding received from the European Union's Horizon 2020 research and innovation programme [grant agreement number 825925]. MAT is financially supported by the Dutch Arthritis Society (LLP22).

Conflict of Interest

CLM and CS are named inventors on the patent for NPgel, KB is named inventor on the patent for the albumin/ hyaluronan hydrogel and employee of TETEC. K.I. is CSO of NC Biomatrix B,V., a company developing dNCM as a commercial product, which holds a licence to the IP for its production process [US 11,607,473 B2 & EP 3 402 542 B1]. Please note that all analysis, interpretation of data and writing of the manuscript has been performed by the authors and companies associated had no control.

References

Aguiar DJ, Johnson SL, Oegema TR (1999) Notochordal cells interact with nucleus pulposus cells: Regulation of proteoglycan synthesis. Exp Cell Res 246: 129-137. DOI: 10.1006/excr.1998.4287.

Alini M, Eisenstein SM, Ito K, Little C, Kettler AA, Masuda K, Melrose J, Ralphs J, Stokes I, Wilke HJ (2008) Are animal models useful for studying human disc disorders/degeneration? Eur Spine J 17: 2-19. DOI: 10.1007/s00586-007-0414-y.

Arkesteijn ITM, Smolders LA, Spillekom S, Riemers FM, Potier E, Meij BP, Ito K, Tryfonidou MA (2015) Effect of coculturing canine notochordal, nucleus pulposus and mesenchymal stromal cells for intervertebral disc regeneration. Arthritis Res Ther 17: 60. DOI: 10.1186/s13075-015-0569-6.

Arkesteijn ITM, Potier E, Ito K (2017) The Regenerative Potential of Notochordal Cells in a Nucleus Pulposus Explant. Global Spine J 7: 14-20. DOI: 10.1055/s-0036-1583174.

Bach FC, Poramba-Liyanage DW, Riemers FM, Guicheux J, Camus A, Iatridis JC, Chan D, Ito K, Le Maitre CL, Tryfonidou MA (2022) Notochordal Cell-Based Treatment Strategies and Their Potential in Intervertebral Disc Regeneration. Front Cell Dev Biol 9: 780749. DOI: 10.3389/fcell.2021.780749.

Bach FC, Tellegen AR, Beukers M, Miranda-Bedate A, Teunissen M, de Jong WAM, de Vries SAH, Creemers LB, Benz K, Meij BP, Ito K, Tryfonidou MA (2018) Biologic canine and human intervertebral disc repair by notochordal cell-derived matrix: from bench towards bedside. Oncotarget 9: 26507-26526. DOI: 10.18632/oncotarget.25476.

Bagwell J, Norman J, Ellis K, Peskin B, Hwang J, Ge X, Nguyen SV, McMenamin SK, Stainier DY, Bagnat M (2020) Notochord vacuoles absorb compressive bone growth during zebrafish spine formation. eLife 9: e51221. DOI: 10.7554/eLife.51221.

Bai XD, Li XC, Chen JH, Guo ZM, Hou LS, Wang DL, He Q, Ruan DK (2017) * Coculture with Partial Digestion Notochordal Cell-Rich Nucleus Pulposus Tissue Activates Degenerative Human Nucleus Pulposus Cells. Tissue Eng Part A 23: 837-846. DOI: 10.1089/ten.TEA.2016.0428.

Basatvat S, Bach FC, Barcellona MN, Binch AL, Buckley CT, Bueno B, Chahine NO, Chee A, Creemers LB, Dudli S, Fearing B, Ferguson SJ, Gansau J, Gantenbein B, Gawri R, Glaeser JD, Grad S, Guerrero J, Haglund L, Hernandez PA, Hoyland JA, Huang C, Iatridis JC, Illien-Junger S, Jing L, Kraus P, Laagland LT, Lang G, Leung V, Li Z, Lufkin T, van Maanen JC, McDonnell EE, Panebianco CJ, Presciutti SM, Rao S, Richardson SM, Romereim S, Schmitz TC, Schol J, Setton L, Sheyn D, Snuggs JW, Sun Y, Tan X, Tryfonidou MA, Vo N, Wang D, Williams B, Williams R, Yoon ST, Le Maitre CL (2023) Harmonization and standardization of nucleus pulposus cell extraction and culture methods. JOR Spine 6: e1238. DOI: 10.1002/jsp2.1238.

Baskin JM, Prescher JA, Laughlin ST, Agard NJ, Chang PV, Miller IA, Lo A, Codelli JA, Bertozzi CR (2007) Copper-free click chemistry for dynamic in vivo imaging. Proc Natl Acad Sci U S A 104: 16793-16797. DOI: 10.1073/pnas.0707090104.

Benz K, Freudigmann C, Müller J, Wurst H, Albrecht D, Badke A, Gaissmaier C, Mollenhauer J (2010) A Polyethylene Glycol-Crosslinked Serum Albumin/Hyaluronan Hydrogel for the Cultivation of Chondrogenic Cell Types. Adv Eng Mater 12: B539-B551. DOI: 10.1002/ADEM.201080028.

Benz K, Stippich C, Fischer L, Möhl K, Weber K, Lang J, Steffen F, Beintner B, Gaissmaier C, Mollenhauer

JA (2012) Intervertebral disc cell- and hydrogel-supported and spontaneous intervertebral disc repair in nucleotomized sheep. Eur Spine J 21: 1758-1768. DOI: 10.1007/s00586-012-2443-4.

Bergknut N, Rutges JPHJ, Kranenburg HJC, Smolders LA, Hagman R, Smidt HJ, Lagerstedt AS, Penning LC, Voorhout G, Hazewinkel HAW, Grinwis GCM, Creemers LB, Meij BP, Dhert WJA (2012) The dog as an animal model for intervertebral disc degeneration? Spine 37: 351-358. DOI: 10.1097/BRS.0b013e31821e5665.

Binch A, Snuggs J, Le Maitre CL (2020) Immunohistochemical analysis of protein expression in formalin fixed paraffin embedded human intervertebral disc tissues. JOR Spine 3: e1098. DOI: 10.1002/jsp2.1098.

Bogduk N (2004) Management of chronic low back pain. Med J Aust 180: 79-83. DOI: 10.5694/j.1326-5377.2004.tb05805.x.

Boyes VL, Janani R, Partridge S, Fielding LA, Breen C, Foulkes J, Le Maitre CL, Sammon C (2021) One-pot precipitation polymerisation strategy for tuneable injectable Laponite®-pNIPAM hydrogels: Polymerisation, processability and beyond. Polymer 233: 124201. DOI: 10.1016/J.POLYMER.2021.124201.

Bron JL, Koenderink GH, Everts V, Smit TH (2009) Rheological characterization of the nucleus pulposus and dense collagen scaffolds intended for functional replacement. J Orthop Res 27: 620-626. DOI: 10.1002/jor.20789.

Chan SCW, Ferguson SJ, Gantenbein-Ritter B (2011) The effects of dynamic loading on the intervertebral disc. European Spine Journal: Official Publication of the European Spine Society, the European Spinal Deformity Society, and the European Section of the Cervical Spine Research Society 20: 1796-1812. DOI: 10.1007/s00586-011-1827-1.

Chen JW, Li B, Yang YH, Jiang SD, Jiang LS (2014) Significance of hypoxia in the physiological function of intervertebral disc cells. Crit Rev Eukaryot Gene Expr 24: 193-204. DOI: 10.1615/critreveukaryotgeneexpr.2014010485.

Chen WH, Lo WC, Lee JJ, Su CH, Lin CT, Liu HY, Lin TW, Lin WC, Huang TY, Deng WP (2006) Tissue-engineered intervertebral disc and chondrogenesis using human nucleus pulposus regulated through TGF-beta1 in platelet-rich plasma. J Cell Physiol 209: 744-754. DOI: 10.1002/jcp.20765.

Cornejo MC, Cho SK, Giannarelli C, Iatridis JC, Purmessur D (2015) Soluble factors from the notochordal-rich intervertebral disc inhibit endothelial cell invasion and vessel formation in the presence and absence of pro-inflammatory cytokines. Osteoarthritis Cartilage 23: 487-496. DOI: 10.1016/j.joca.2014.12.010.

de Vries S, Doeselaar MV, Meij B, Tryfonidou M, Ito K (2019) Notochordal Cell Matrix As a Therapeutic Agent for Intervertebral Disc Regeneration. Tissue Eng Part A 25: 830-841. DOI: 10.1089/ten.TEA.2018.0026.

Ellis K, Bagwell J, Bagnat M (2013) Notochord vacuoles are lysosome-related organelles that function in axis and spine morphogenesis. J Cell Biol 200: 667-679. DOI: 10.1083/jcb.201212095.

Foster NE, Anema JR, Cherkin D, Chou R, Cohen SP, Gross DP, Ferreira PH, Fritz JM, Koes BW, Peul W, Turner JA, Maher CG, Lancet Low Back Pain Series Working Group (2018) Prevention and treatment of low back pain: evidence, challenges, and promising directions. Lancet 391: 2368-2383. DOI: 10.1016/S0140-6736(18)30489-6.

Gantenbein-Ritter B, Chan SCW (2012) The evolutionary importance of cell ratio between notochordal and nucleus pulposus cells: an experimental 3-D co-culture study. Eur Spine J 21: S819-S825. DOI: 10.1007/s00586-011-2026-9.

Gantenbein B, Calandriello E, Wuertz-Kozak K, Benneker LM, Keel MJB, Chan SCW (2014) Activation of intervertebral disc cells by co-culture with notochordal cells, conditioned medium and hypoxia. BMC Musculoskelet Disord 15: 422. DOI: 10.1186/1471-2474-15-422.

Guehring T, Nerlich A, Kroeber M, Richter W, Omlor GW (2010) Sensitivity of notochordal disc cells to mechanical loading: an experimental animal study. Eur Spine J 19: 113-121. DOI: 10.1007/s00586-009-1217-0.

Guehring T, Wilde G, Sumner M, Grünhagen T, Karney GB, Tirlapur UK, Urban JPG (2009) Notochordal intervertebral disc cells: sensitivity to nutrient deprivation. Arthritis Rheum 60: 1026-1034. DOI: 10.1002/art.24407.

Hartvigsen J, Hancock MJ, Kongsted A, Louw Q, Ferreira ML, Genevay S, Hoy D, Karppinen J, Pransky G, Sieper J, Smeets RJ, Underwood M, Lancet Low Back Pain Series Working Group (2018) What low back pain is and why we need to pay attention. Lancet 391: 2356-2367. DOI: 10.1016/S0140-6736(18)30480-X.

Hong X, Zhang C, Wang F, Wu XT (2018) Large Cytoplasmic Vacuoles within Notochordal Nucleus Pulposus Cells: A Possible Regulator of Intracellular Pressure That Shapes the Cytoskeleton and Controls Proliferation. Cells Tissues Organs 206: 9-15. DOI: 10.1159/000493258.

Humphreys MD, Ward L, Richardson SM, Hoyland JA (2018) An optimized culture system for notochordal cell expansion with retention of phenotype. JOR Spine 1: e1028. DOI: 10.1002/jsp2.1028.

Hunter CJ, Bianchi S, Cheng P, Muldrew K (2007) Osmoregulatory function of large vacuoles found in notochordal cells of the intervertebral disc running title: an osmoregulatory vacuole. Mol Cell Biomech 4: 227-237.

Hunter CJ, Matyas JR, Duncan NA (2003) The three-dimensional architecture of the notochordal nucleus pulposus: novel observations on cell structures in the canine intervertebral disc. J Anat 202: 279-291. DOI: 10.1046/j.1469-7580.2003.00162.x.

Iatridis JC, Setton LA, Weidenbaum M, Mow VC (1997) Alterations in the mechanical behavior of the human lumbar nucleus pulposus with degeneration and aging.

J Orthop Res 15: 318-322. DOI: 10.1002/jor.1100150224.

Iatridis JC, Weidenbaum M, Setton LA, Mow VC (1996) Is the nucleus pulposus a solid or a fluid? Mechanical behaviors of the nucleus pulposus of the human intervertebral disc. Spine 21: 1174-1184. DOI: 10.1097/00007632-199605150-00009.

Kim JH, Deasy BM, Seo HY, Studer RK, Vo NV, Georgescu HI, Sowa GA, Kang JD (2009) Differentiation of intervertebral notochordal cells through live automated cell imaging system in vitro. Spine 34: 2486-2493. DOI: 10.1097/BRS.0b013e3181b26ed1.

Korecki CL, MacLean JJ, Iatridis JC (2008) Dynamic compression effects on intervertebral disc mechanics and biology. Spine 33: 1403-1409. DOI: 10.1097/BRS.0b013e318175cae7.

Korecki CL, Taboas JM, Tuan RS, Iatridis JC (2010) Notochordal cell conditioned medium stimulates mesenchymal stem cell differentiation toward a young nucleus pulposus phenotype. Stem Cell Research & Therapy 1: 18. DOI: 10.1186/scrt18.

Kuwaki K, Tseng YL, Dor FJMF, Shimizu A, Houser SL, Sanderson TM, Lancos CJ, Prabharasuth DD, Cheng J, Moran K, Hisashi Y, Mueller N, Yamada K, Greenstein JL, Hawley RJ, Patience C, Awwad M, Fishman JA, Robson SC, Schuurman HJ, Sachs DH, Cooper DKC (2005) Heart transplantation in baboons using alpha1,3-galactosyltransferase gene-knockout pigs as donors: initial experience. Nature Medicine 11: 29-31. DOI: 10.1038/nm1171.

Laagland LT, Bach FC, Creemers LB, Le Maitre CL, Poramba-Liyanage DW, Tryfonidou MA (2022) Hyperosmolar expansion medium improves nucleus pulposus cell phenotype. JOR Spine 5: e1219. DOI: 10.1002/jsp2.1219.

Lai L, Prather RS (2002) Progress in producing knockout models for xenotransplantation by nuclear transfer. Annals of Medicine 34: 501-506. DOI: 10.1080/078538902321117706.

Le Maitre CL, Fotheringham AP, Freemont AJ, Hoyland JA (2009) Development of an in vitro model to test the efficacy of novel therapies for IVD degeneration. Journal of Tissue Engineering and Regenerative Medicine 3: 461-469. DOI: 10.1002/term.180.

Leung VYL, Chan WCW, Hung SC, Cheung KMC, Chan D (2009) Matrix remodeling during intervertebral disc growth and degeneration detected by multichromatic FAST staining. J Histochem Cytochem 57: 249-256. DOI: 10.1369/jhc.2008.952184.

Luoma K, Riihimäki H, Luukkonen R, Raininko R, Viikari-Juntura E, Lamminen A (2000) Low back pain in relation to lumbar disc degeneration. Spine 25: 487-492. DOI: 10.1097/00007632-200002150-00016.

Ma K, Wu Y, Wang B, Yang S, Wei Y, Shao Z (2013) Effect of a synthetic link N peptide nanofiber scaffold on the matrix deposition of aggrecan and type II collagen in rabbit notochordal cells. J Mater Sci Mater Med 24: 405-415. DOI: 10.1007/s10856-012-4811-3.

Maetzel A, Li L (2002) The economic burden of low back pain: a review of studies published between 1996 and 2001. Best Pract Res Clin Rheumatol 16: 23-30. DOI: 10.1053/berh.2001.0204.

Maroudas A, Stockwell RA, Nachemson A, Urban J (1975) Factors involved in the nutrition of the human lumbar intervertebral disc: cellularity and diffusion of glucose in vitro. J Anat 120: 113-130.

McCann MR, Séguin CA (2016) Notochord Cells in Intervertebral Disc Development and Degeneration. J Dev Biol 4: 3. DOI: 10.3390/jdb4010003.

Minogue BM, Richardson SM, Zeef LA, Freemont AJ, Hoyland JA (2010) Transcriptional profiling of bovine intervertebral disc cells: implications for identification of normal and degenerate human intervertebral disc cell phenotypes. Arthritis Res Ther 12: R22. DOI: 10.1186/ar2929.

NICE (2020) Low back pain and sciatica in over 16s: assessment and management. Available at: https://www.nice.org.uk/guidance/ng59 (Accessed: 23 Sep 2023).

Niemeyer P, Hanus M, Belickas J, László T, Gudas R, Fiodorovas M, Cebatorius A, Pastucha M, Hoza P, Magos K, Izadpanah K, Paša L, Vásárhelyi G, Sisák K, Mohyla M, Farkas C, Kessler O, Kybal S, Spiro R, Köhler A, Kirner A, Trattnig S, Gaissmaier C (2022) Treatment of Large Cartilage Defects in the Knee by Hydrogel-Based Autologous Chondrocyte Implantation: Two-Year Results of a Prospective, Multicenter, Single-Arm Phase III Trial. Cartilage 13: 19476035221085146. DOI: 10.1177/19476035221085146.

Oegema TR Jr (1993) Biochemistry of the intervertebral disc. Clin Sports Med 12: 419-439.

Peroglio M, Grad S, Mortisen D, Sprecher CM, Illien-Jünger S, Alini M, Eglin D (2012) Injectable thermoreversible hyaluronan-based hydrogels for nucleus pulposus cell encapsulation. Eur Spine J 21: S839-S849. DOI: 10.1007/s00586-011-1976-2.

Phillips K, Ch'ien APY, Norwood BR, Smith C (2003) Chronic low back pain management in primary care. Nurse Pract 28: 26-31. DOI: 10.1097/00006205-200308000-00008.

Phillips KLE, Cullen K, Chiverton N, Michael ALR, Cole AA, Breakwell LM, Haddock G, Bunning RAD, Cross AK, Le Maitre CL (2015) Potential roles of cytokines and chemokines in human intervertebral disc degeneration: interleukin-1 is a master regulator of catabolic processes. Osteoarthritis and Cartilage 23: 1165-1177. DOI: 10.1016/j.joca.2015.02.017.

Potier E, de Vries S, van Doeselaar M, Ito K (2014) Potential application of notochordal cells for intervertebral disc regeneration: an in vitro assessment. Eur Cell Mater 28: 68-81. DOI: 10.22203/ecm.v028a06.

Potier E, Ito K (2014) Using notochordal cells of developmental origin to stimulate nucleus pulposus cells and bone marrow stromal cells for intervertebral disc regenera-

tion. Eur Spine J 23: 679-688. DOI: 10.1007/s00586-013-3107-8.

Purmessur D, Guterl CC, Cho SK, Cornejo MC, Lam YW, Ballif BA, Laudier JCI, Iatridis JC (2013) Dynamic pressurization induces transition of notochordal cells to a mature phenotype while retaining production of important patterning ligands from development. Arthritis Res Ther 15: R122. DOI: 10.1186/ar4302.

Qaseem A, Wilt TJ, McLean RM, Forciea MA, Clinical Guidelines Committee of the American College of Physicians, Denberg TD, Barry MJ, Boyd C, Chow RD, Fitterman N, Harris RP, Humphrey LL, Vijan S (2017) Noninvasive Treatments for Acute, Subacute, and Chronic Low Back Pain: A Clinical Practice Guideline From the American College of Physicians. Ann Intern Med 166: 514-530. DOI: 10.7326/M16-2367.

Risbud MV, Schaer TP, Shapiro IM (2010) Toward an understanding of the role of notochordal cells in the adult intervertebral disc: from discord to accord. Dev Dyn 239: 2141-2148. DOI: 10.1002/dvdy.22350.

Risbud MV, Shapiro IM (2011) Notochordal cells in the adult intervertebral disc: new perspective on an old question. Crit Rev Eukaryot Gene Expr 21: 29-41. DOI: 10.1615/critreveukargeneexpr.v21.i1.30.

Roughley PJ (2004) Biology of intervertebral disc aging and degeneration: involvement of the extracellular matrix. Spine 29: 2691-2699. DOI: 10.1097/01.brs.0000146101.53784.b1.

Sachs DH (1994) The pig as a potential xenograft donor. Veterinary Immunology and Immunopathology 43: 185-191. DOI: 10.1016/0165-2427(94)90135-x.

Saggese T, Thambyah A, Wade K, McGlashan SR (2020) Differential Response of Bovine Mature Nucleus Pulposus and Notochordal Cells to Hydrostatic Pressure and Glucose Restriction. Cartilage 11: 221-233. DOI: 10.1177/1947603518775795.

Sakai D, Andersson GBJ (2015) Stem cell therapy for intervertebral disc regeneration: obstacles and solutions. Nat Rev Rheumatol 11: 243-256. DOI: 10.1038/nrrheum.2015.13.

Schmitz TC, van Doeselaar M, Tryfonidou MA, Ito K (2022) Detergent-Free Decellularization of Notochordal Cell-Derived Matrix Yields a Regenerative, Injectable, and Swellable Biomaterial. ACS Biomater Sci Eng 8: 3912-3923. DOI: 10.1021/acsbiomaterials.2c00790.

Sheyn D, Ben-David S, Tawackoli W, Zhou Z, Salehi K, Bez M, De Mel S, Chan V, Roth J, Avalos P, Giaconi JC, Yameen H, Hazanov L, Seliktar D, Li D, Gazit D, Gazit Z (2019) Human iPSCs can be differentiated into notochordal cells that reduce intervertebral disc degeneration in a porcine model. Theranostics 9: 7506-7524. DOI: 10.7150/thno.34898.

Shin JS, Kim JM, Kim JS, Min BH, Kim YH, Kim HJ, Jang JY, Yoon IH, Kang HJ, Kim J, Hwang ES, Lim DG, Lee WW, Ha J, Jung KC, Park SH, Kim SJ, Park CG (2015) Long-term control of diabetes in immunosuppressed nonhuman primates (NHP) by the transplantation of adult porcine islets. American Journal of Transplantation: Official Journal of the American Society of Transplantation and the American Society of Transplant Surgeons 15: 2837-2850. DOI: 10.1111/ajt.13345.

Snuggs JW, Emanuel KS, Rustenburg C, Janani R, Partridge S, Sammon C, Smit TH, Le Maitre CL (2023) Injectable biomaterial induces regeneration of the intervertebral disc in a caprine loaded disc culture model. Biomater Sci 11: 4630-4643. DOI: 10.1039/d3bm00150d.

Soukane DM, Shirazi-Adl A, Urban JPG (2005) Analysis of nonlinear coupled diffusion of oxygen and lactic acid in intervertebral discs. J Biomech Eng 127: 1121-1126. DOI: 10.1115/1.2073674.

Spillekom S, Smolders LA, Grinwis GCM, Arkesteijn ITM, Ito K, Meij BP, Tryfonidou MA (2014) Increased osmolarity and cell clustering preserve canine notochordal cell phenotype in culture. Tissue Eng Part C Methods 20: 652-662. DOI: 10.1089/ten.TEC.2013.0479.

Steffens D, Maher CG, Pereira LSM, Stevens ML, Oliveira VC, Chapple M, Teixeira-Salmela LF, Hancock MJ (2016) Prevention of Low Back Pain: A Systematic Review and Meta-analysis. JAMA Intern Med 176: 199-208. DOI: 10.1001/jamainternmed.2015.7431.

Thompson P, Badell IR, Lowe M, Cano J, Song M, Leopardi F, Avila J, Ruhil R, Strobert E, Korbutt G, Rayat G, Rajotte R, Iwakoshi N, Larsen CP, Kirk AD (2011) Islet xenotransplantation using gal-deficient neonatal donors improves engraftment and function. American Journal of Transplantation: Official Journal of the American Society of Transplantation and the American Society of Transplant Surgeons 11: 2593-2602. DOI: 10.1111/j.1600-6143.2011.03720.x.

Thorpe AA, Dougill G, Vickers L, Reeves ND, Sammon C, Cooper G, Le Maitre CL. (2017). Thermally triggered hydrogel injection into bovine intervertebral disc tissue explants induces differentiation of mesenchymal stem cells and restores mechanical function. Acta Biomater. 8. pii: S1742-7061(17)30172-1. DOI: 10.1016/j.actbio.2017.03.010.

Thorpe AA, Freeman C, Farthing P, Callaghan J, Hatton PV, Brook IM, Sammon C, Le Maitre CL (2018) *In vivo* safety and efficacy testing of a thermally triggered injectable hydrogel scaffold for bone regeneration and augmentation in a rat model. Oncotarget 9: 18277-18295. DOI: 10.18632/oncotarget.24813.

Thorpe AA, Boyes VL, Sammon C, Le Maitre CL (2016) Thermally triggered injectable hydrogel, which induces mesenchymal stem cell differentiation to nucleus pulposus cells: Potential for regeneration of the intervertebral disc. Acta Biomater 36: 99-111. DOI: 10.1016/j.actbio.2016.03.029.

Traeger AC, Buchbinder R, Elshaug AG, Croft PR, Maher CG (2019) Care for low back pain: can health sys-

tems deliver? Bull World Health Organ 97: 423-433. DOI: 10.2471/BLT.18.226050.

Urban JP, Holm S, Maroudas A (1978) Diffusion of small solutes into the intervertebral disc: as in vivo study. Biorheology 15: 203-221. DOI: 10.3233/bir-1978-153-409.

Urban JPG, Roberts S (2003) Degeneration of the intervertebral disc. Arthritis Res Ther 5: 120-130. DOI: 10.1186/ar629.

Vickers L, Thorpe AA, Snuggs J, Sammon C, Le Maitre CL (2019) Mesenchymal stem cell therapies for intervertebral disc degeneration: Consideration of the degenerate niche. JOR Spine 2: e1055. DOI: 10.1002/jsp2.1055.

Wang F, Gao ZX, Cai F, Sinkemani A, Xie ZY, Shi R, Wei JN, Wu XT (2017) Formation, function, and exhaustion of notochordal cytoplasmic vacuoles within intervertebral disc: current understanding and speculation. Oncotarget 8: 57800-57812. DOI: 10.18632/oncotarget.18101.

Wilke HJ, Neef P, Caimi M, Hoogland T, Claes LE (1999) New in vivo measurements of pressures in the intervertebral disc in daily life. Spine 24: 755-762. DOI: 10.1097/00007632-199904150-00005.

Williams RJ, Tryfonidou MA, Snuggs JW, Le Maitre CL (2021) Cell sources proposed for nucleus pulposus regeneration. JOR Spine 4: e1175. DOI: 10.1002/jsp2.1175.

Williams RJ, Laagland LT, Bach FC, Ward L, Chan W, Tam V, Medzikovic A, Basatvat S, Paillat L, Vedrenne N, Snuggs JW, Poramba-Liyanage DW, Hoyland JA, Chan D, Camus A, Richardson SM, Tryfonidou MA, Le Maitre CL. (2023) Recommendations for intervertebral disc notochordal cell investigation: From isolation to characterization. JOR Spine 6(3):e1272. DOI: 10.1002/jsp2.1272.

Yurube T, Hirata H, Kakutani K, Maeno K, Takada T, Zhang Z, Takayama K, Matsushita T, Kuroda R, Kurosaka M, Nishida K (2014) Notochordal cell disappearance and modes of apoptotic cell death in a rat tail static compression-induced disc degeneration model. Arthritis Res Ther 16: R31. DOI: 10.1186/ar4460.

Editor's note: The Scientific Editor responsible for this paper was Sibylle Grad.